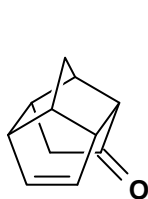


# 1

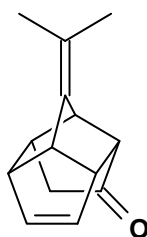
## Introduction

### 1.1. Aim of study

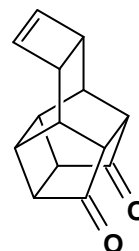
The aim of this study was to synthesise cage alkenes and to investigate the polymerisability of these compounds with well-defined ruthenium carbene ring-opening metathesis polymerisation (ROMP) catalysts. It is well established<sup>1-4</sup> that cyclic alkenes, norbornene, and norbornene derivatives are useful substrates for ROMP. Although examples of polymers incorporating cage structures are known,<sup>5-10</sup> a thorough literature search revealed only one example<sup>11</sup> of a cage alkene incorporated into the backbone of a ROMP polymer. It was concluded that a study of the synthetic utility of cage alkenes in the ROMP reaction could be a worthwhile activity. To this end the ketoalkene **1** and some simple derivatives were prepared. Attempts were made to synthesise the cage alkene **2**, and the structurally related cage alkene **3**, was selected from the literature.



**1**



**2**

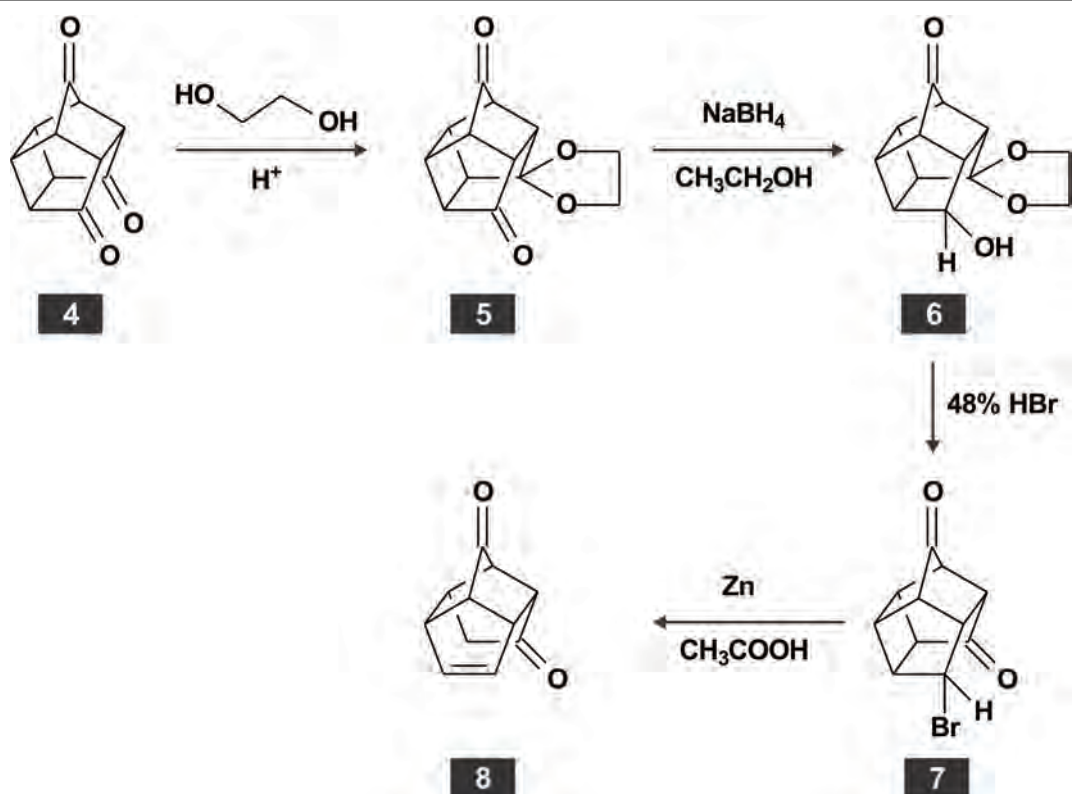


**3**

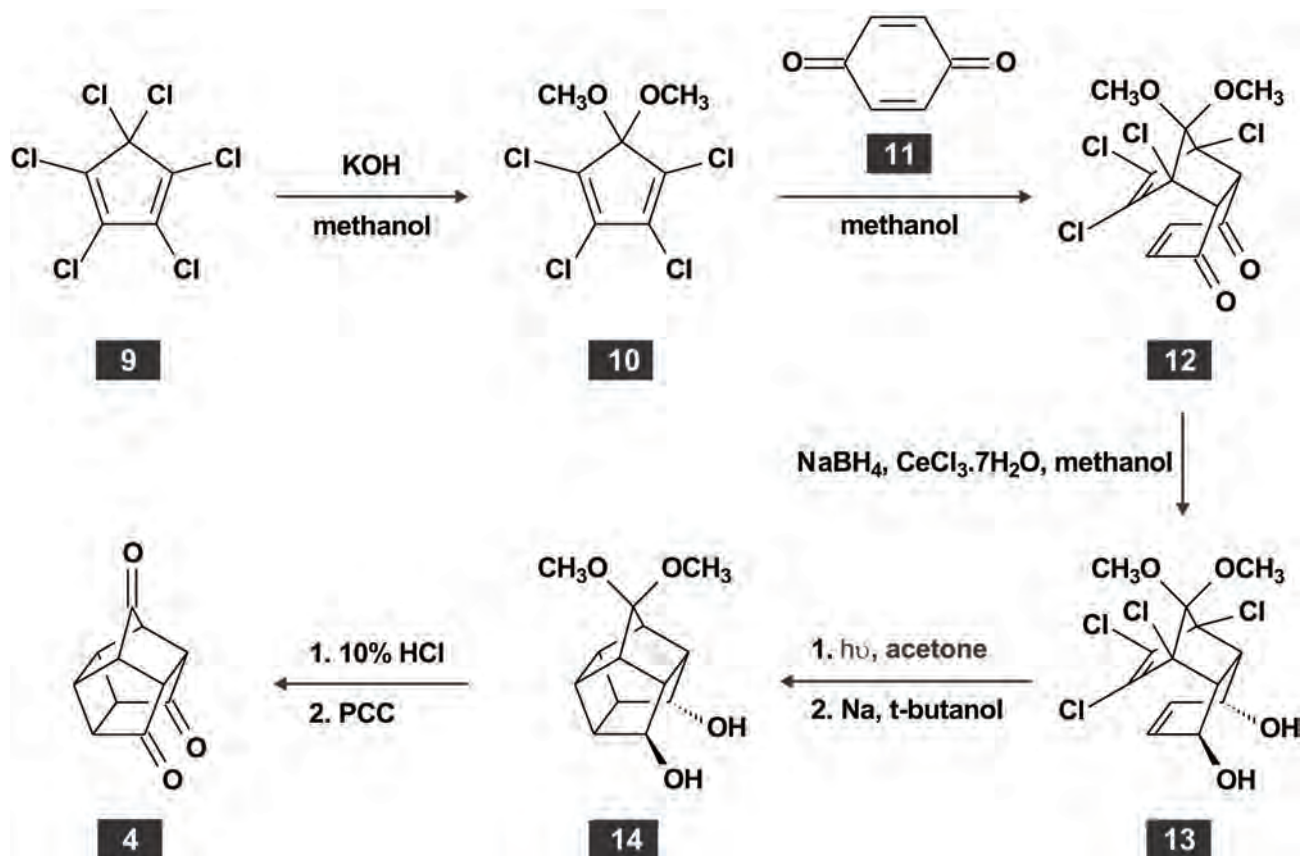
### 1.2. Prelude

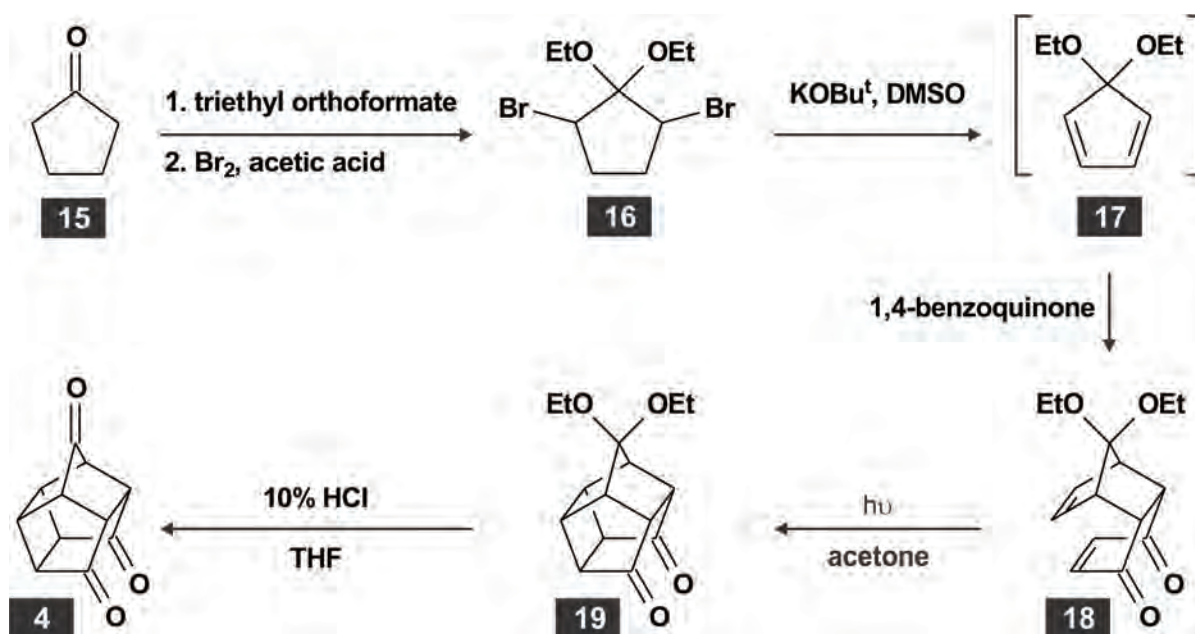
Initially the synthesis of the cage alkene **8** was investigated (**Scheme 1.1**). This compound was selected for its structural similarity to the ketoalkene **1** that could facilitate comparison of their chemical behaviour.

The synthesis route<sup>12-13</sup> to pentacyclo[5.4.0.0<sup>2,6</sup>.0<sup>3,10</sup>.0<sup>5,9</sup>]undecane-4,8,11-trione (**4**) consists of seven steps and involves the use of 1,2,3,4,5,5-hexachlorocyclopenta-1,3-diene (**9**, **Scheme 1.2**), which is classified as a persistent organic pollutant (POP). Attempts were made to shorten the synthesis of **4**. For this purpose, two alternative synthesis routes were thoroughly investigated. **Scheme 1.3** depicts the synthesis<sup>14</sup> of **4** using the *in situ* generated diene **17**. This method was tedious and produced low yields. The method was not suitable to produce large amounts of a starting material for this project.



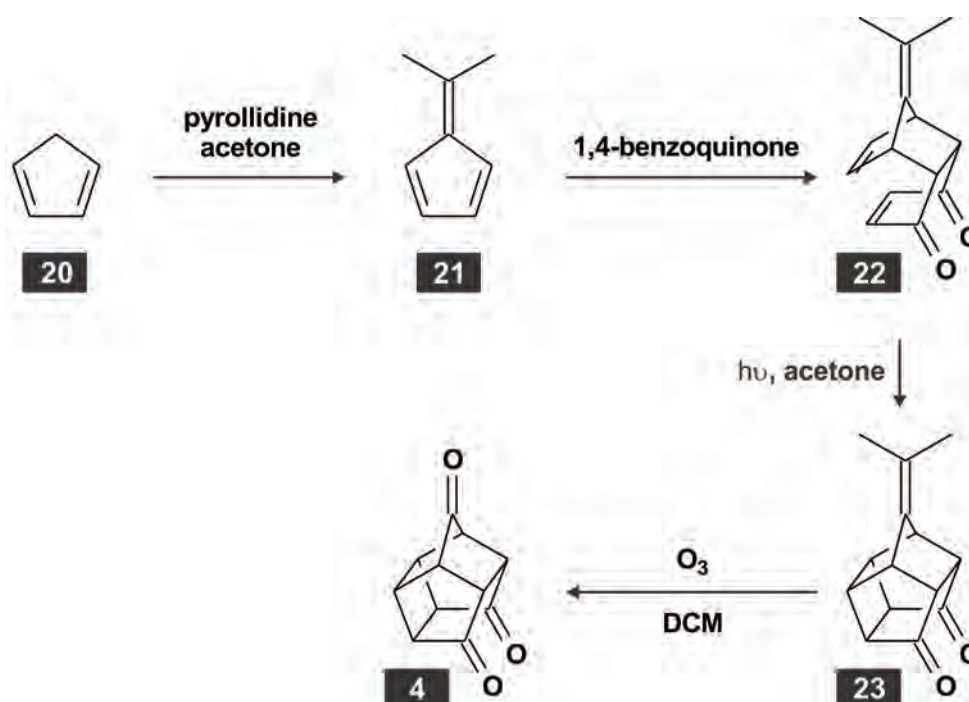
Scheme 1.1: Initially envisaged synthesis scheme.

Scheme 1.2<sup>12-13</sup>: Preparation of trione 4 from 9.



**Scheme 1.3**<sup>14</sup>: Preparation of trione **4** through the *in situ* generated diene **17**.

The second route to **4** is shown in **Scheme 1.4**. The route involves the ozonolysis of 4-isopropylidene-pentacyclo[5.4.0.0<sup>2,6</sup>.0<sup>3,10</sup>.0<sup>5,9</sup>]undecane-8,11-dione (**23**). This approach shortened the synthesis of **4** to four steps. This synthesis approach was convenient and suitable for the large scale synthesis of starting material.



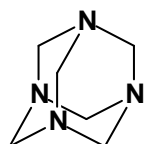
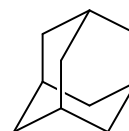
**Scheme 1.4**: Preparation of **4** through ozonolysis of **23**.

The results of a literature search indicated that the chemistry of **23** had not been the subject of investigation. As a result, I opted to focus my further work on the synthesis and chemistry of this compound. To increase the structural diversity of compounds used in the study, I added the cage alkene **3**.

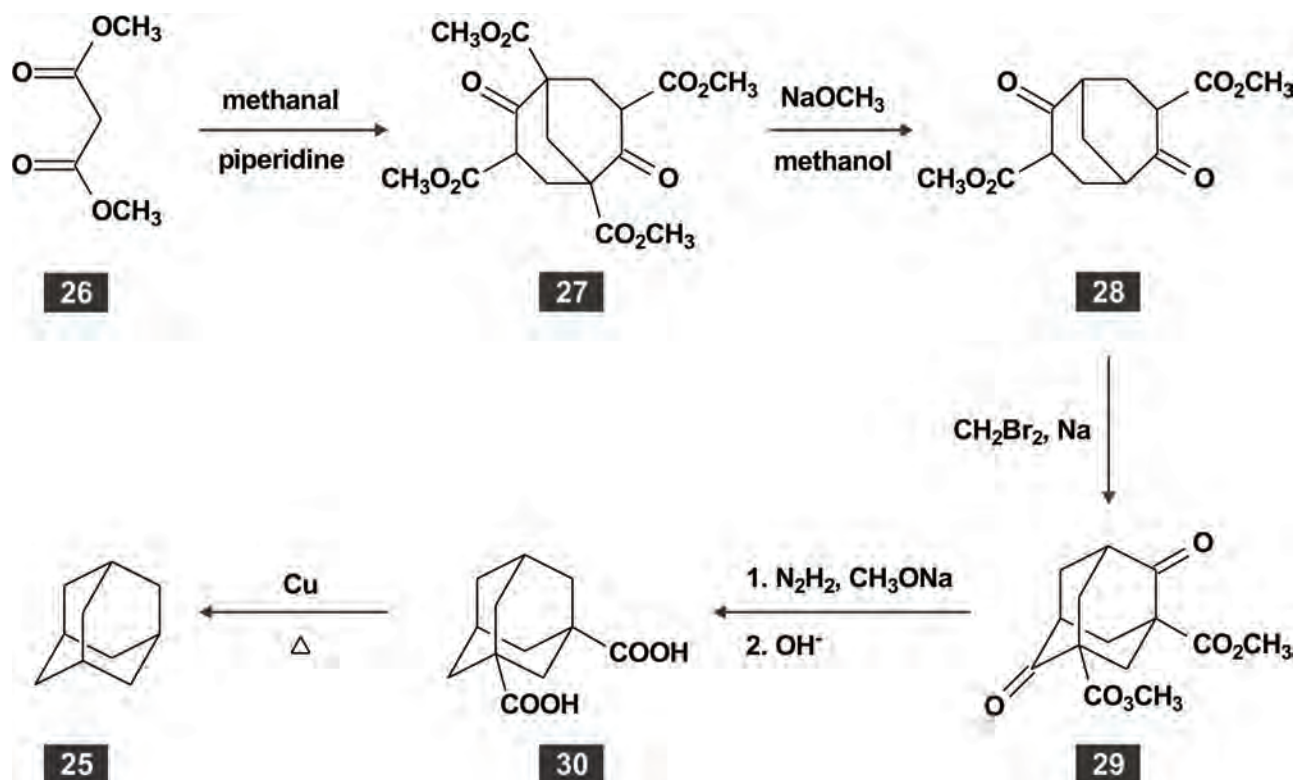
### 1.3. Brief overview of polycyclic cage compounds

A cage compound is defined<sup>15</sup> as a polycyclic compound having the shape of a cage. Historically, these compounds have been attractive synthetic targets owing to their aesthetically pleasing geometry and the associated intellectual challenge.<sup>16-17</sup> Cage compounds exhibit unique structural properties that distinguish them from acyclic systems. They are usually strained as expressed through their longer than normal framework carbon-carbon  $\sigma$ -bonds and C–C–C bond angles that deviate noticeably from the norm.<sup>18</sup> These molecules are characterised by rigid carbon frameworks that manifest as locked conformations with bond distances and bond angles that can be estimated reliably.<sup>19</sup> The unique structural characteristics of cage molecules have made them ideal model substrates in mechanistic studies.<sup>20-25</sup> In modern times, cage compounds are far from scientific curiosities. In addition to their application in mechanistic studies they have potential medicinal applications,<sup>26-29</sup> are used in the synthesis of novel fused ring systems,<sup>30</sup> serve as the basis of interesting non-natural amino acids<sup>31-33</sup> and peptides,<sup>34</sup> are incorporated into polymers,<sup>5-10</sup> and have been investigated as potential explosives.<sup>13,35</sup>

It seems that hexamine (**24**) was the first synthetically-produced polycyclic cage compound.<sup>36</sup> Although this compound was already synthesised in 1860, its caged nature was only recognised in 1895.<sup>37</sup> Hexamine is still an important industrial chemical manufactured from ammonia and formaldehyde.<sup>38</sup> The all-carbon analogue of hexamine was discovered in 1933 when a white substance crystallised from a sample of crude oil taken in former Czechoslovakia.<sup>39</sup> The substance was named adamantane (**25**) because of its structural similarity to diamond.

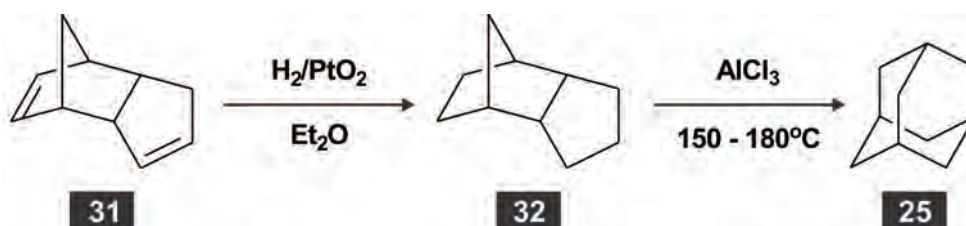
**24****25**

The first adamantane analogue was reported by Böttger in 1937.<sup>40</sup> Adamantane was subsequently synthesised (**Scheme 1.5**) by Prelog and Seiwert in 1941.<sup>41</sup>



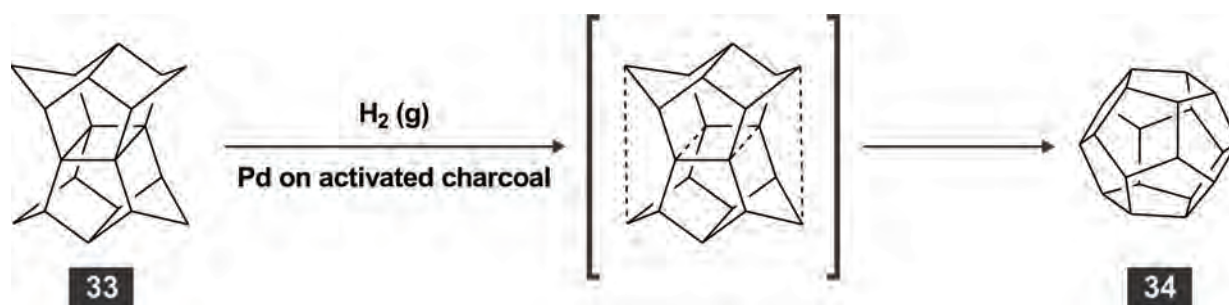
**Scheme 1.5**<sup>41</sup>: Synthesis of adamantane.

This and similar attempts to synthesise adamantane may be regarded as the first steps in the development of polycyclic cage chemistry. Unfortunately, these methods of synthesis produced adamantane in low yields. Further investigations of the chemistry of adamantane demanded a suitable synthetic route to the compound. The discovery of such a method followed in 1957 with the synthesis of adamantane starting from cyclopentadiene (**Scheme 1.6**).<sup>42</sup>



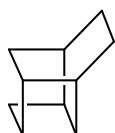
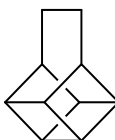
**Scheme 1.6**<sup>42</sup>: Synthesis of adamantane by hydrogenation and rearrangement.

The synthesis of adamantane by rearrangement heralded a new era in the development of cage chemistry since this strategy could also be applied to the synthesis of other complex hydrocarbons. The approach is perhaps best exemplified by the successful synthesis of dodecahedrane (**34**) from pagodane (**33**, **Scheme 1.7**).<sup>43</sup>



**Scheme 1.7**<sup>43</sup>: Synthesis of dodecahedrane from pagodane.

Until about 1960, the chemistry of cage compounds was largely confined to adamantane. Thereafter, many different types of cage compounds were synthesised and a recognisable field emerged.<sup>44</sup> Some examples of cage compounds include twistane (**35**),<sup>45</sup> triprismane (**36**),<sup>46</sup> cubane (**37**),<sup>47</sup> basketane (**38**),<sup>48-49</sup> homopentaprismane (**39**)<sup>50-51</sup> and pentaprismane (**40**).<sup>52</sup> Successful synthesis of these compounds showed that organic chemists could synthesise in a rational way compounds that were foreign to nature.<sup>53</sup>

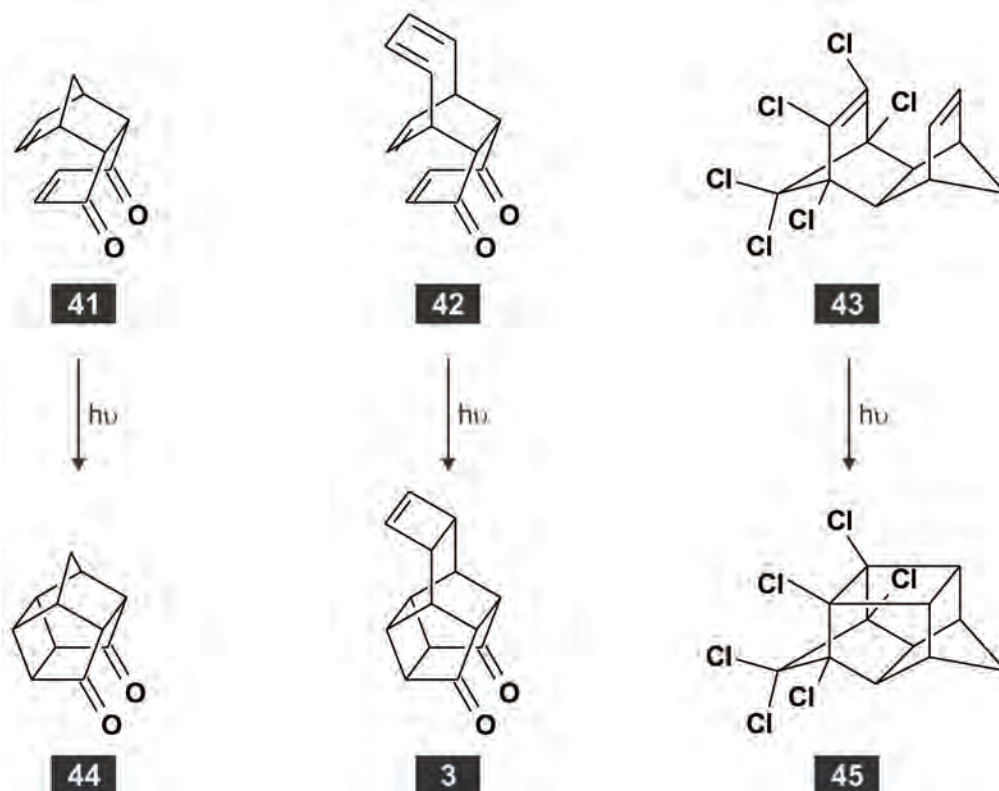
**35****36****37****38****39****40**

#### 1.4. Cage molecules by irradiation of Diels-Alder adducts

The first examples of cage-like molecules produced by irradiation of Diels-Alder adducts were reported in 1958.<sup>54-55</sup> Cage molecules **44**, **3**, and **45** were formed from adducts **41**, **42**, and **43** (**Scheme 1.8**).

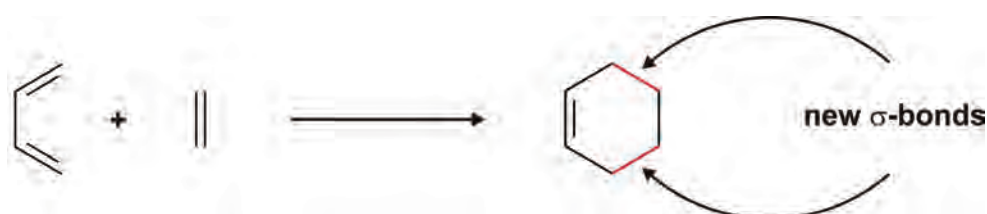
##### 1.4.1. The Diels-Alder reaction

The Diels-Alder reaction (**Scheme 1.9**) is a stereospecific cycloaddition of a  $\pi$ -system with  $2\pi$  electrons (dienophile) to a conjugated  $\pi$ -system with  $4\pi$  electrons (diene). The reaction is of wide scope and has been extensively used in organic synthesis.<sup>56</sup> There is general agreement that the



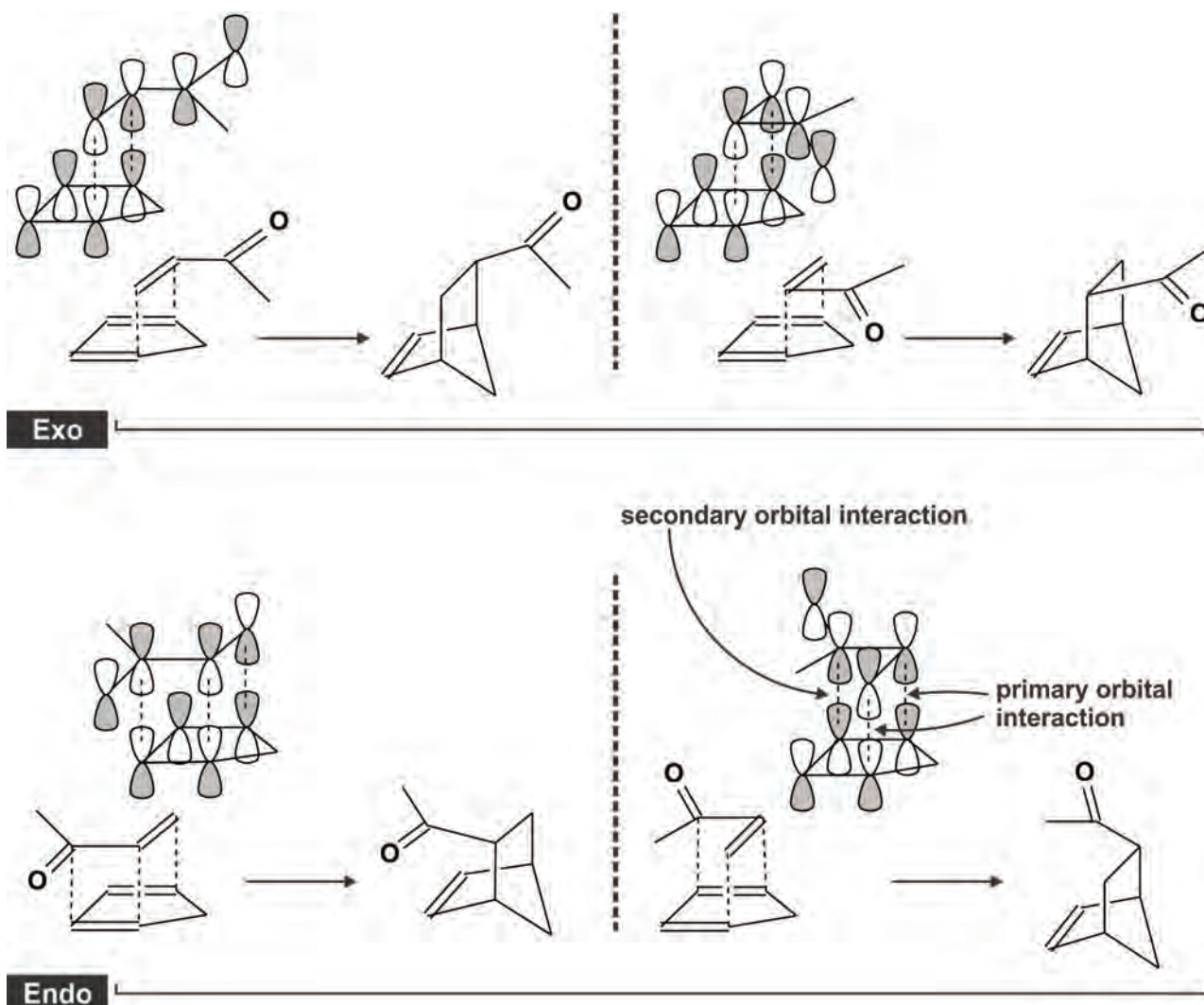
**Scheme 1.8**<sup>42</sup>: Synthesis of cage molecules by irradiation of Diels-Alder adducts.

reaction between the diene and dienophile usually is a concerted process.<sup>57-58</sup> In such cases, the configurations of the double bonds of the diene and dienophile are conserved in the adduct in accordance with the rules of Woodward and Hoffmann.<sup>59</sup>



**Scheme 1.9**: The simplest example of a Diels-Alder reaction.<sup>60</sup>

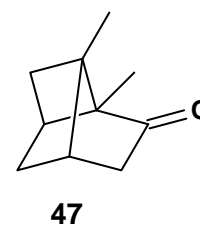
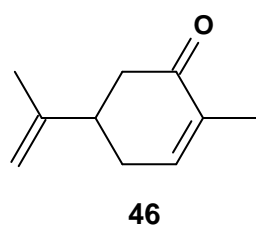
The dienophile can adopt two possible stereochemical orientations towards a cyclic diene (**Scheme 1.10**). Experimentally, a preference for the *endo*-adduct is usually observed even though this is the sterically more congested product.<sup>61</sup> This preference has been ascribed<sup>62-63</sup> to secondary interactions between the orbitals of the diene and dienophile. **Scheme 1.10** shows that stabilising overlap of the  $\pi$ -orbitals of the diene and the  $\pi$ -orbitals of the carbonyl group of the dienophile is only possible in the *endo*-transition state. The *endo*-adduct is the kinetically-controlled product and will ultimately revert to the more stable *exo*-adduct if the reaction is reversible.



**Scheme 1.10:** Formation of *exo*- and *endo*-adducts.<sup>64</sup>

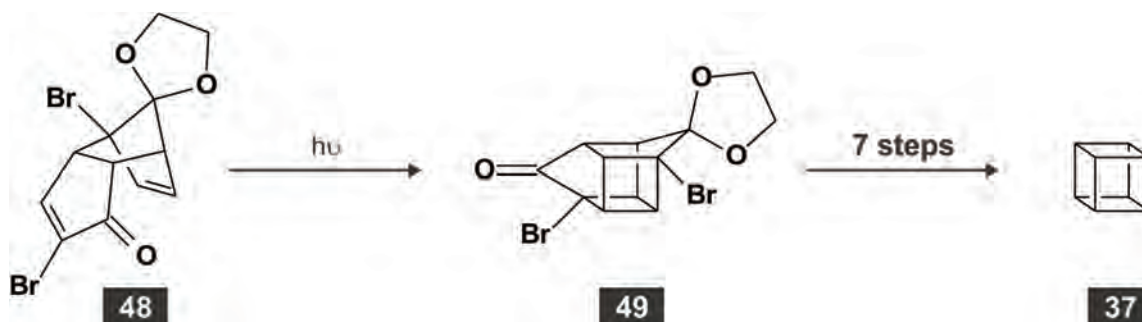
### 1.4.2. Photochemical [2 + 2] cycloadditions

The first example of a photochemical [2 + 2] cycloaddition was reported<sup>65</sup> in 1908 after the Italian photochemist Giacomo Luigi Ciamician observed the conversion of carvone (**46**) to carvone camphor (**47**) on exposure to sunlight for an extended period of time. There was some disagreement as to the structure of the product and the result was only confirmed in 1957.<sup>66</sup>



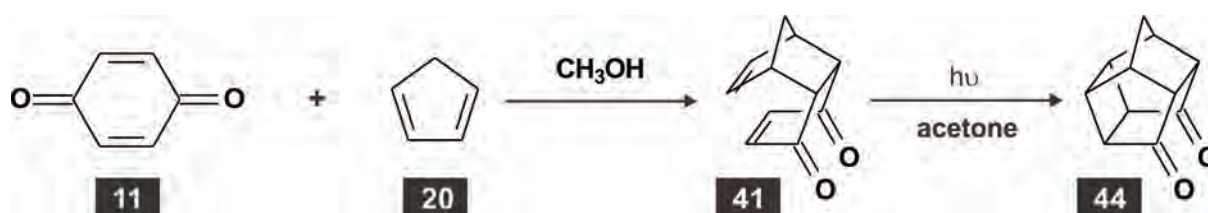


Photocycloadditions have been used as key steps in a number of complex syntheses.<sup>67</sup> The photochemical [2 + 2] cycloaddition of alkenes is especially efficient in rigid polycyclic systems that hold the double bonds in close proximity. The groundbreaking synthesis of cubane (**37**) illustrates the use of an intramolecular [2 + 2] photocyclisation in the construction of a cage compound (**Scheme 1.11**). It is clear that the construction of the cage framework would be extremely difficult without the photocyclisation step.



**Scheme 1.11**<sup>47</sup>: Use of photocyclisation in the synthesis of cubane.

Photocyclisation of the *endo*-adduct of 1,3-cyclopentadiene (**20**) and 1,4-benzoquinone (**11**) is another classic example of the construction of a cage compound (**Scheme 1.12**).<sup>55</sup>



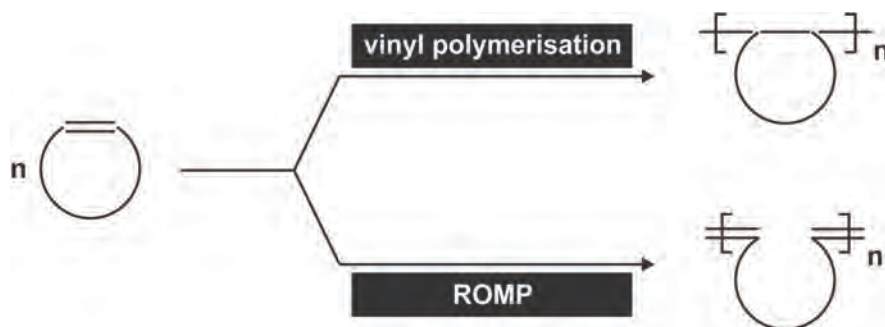
**Scheme 1.12**<sup>68</sup>: Synthesis of pentacyclo[5.4.0.0<sup>2,6</sup>.0<sup>3,10</sup>.0<sup>5,9</sup>]undecane-8,11-dione.

It has been established that most photocyclisation reactions involve a triplet excited state and proceeds through a diradical mechanism.<sup>69</sup> It was concluded from a recent computational study that the photocyclisation of **41** might also proceed through this mechanism rather than through a concerted [2 + 2] cycloaddition.<sup>70</sup>

## 1.5. Ring-opening metathesis polymerisation

### 1.5.1. Introduction

The polymerisation of cycloalkenes has been extensively reviewed in the literature.<sup>71</sup> Cycloalkenes undergo vinyl polymerisation and ring-opening metathesis polymerisation (ROMP) depending on the catalytic system used (**Scheme 1.13**).<sup>72</sup> In the case of vinyl polymerisation, the product is a polycycloalkene while the ROMP product is a polyalkenamer.

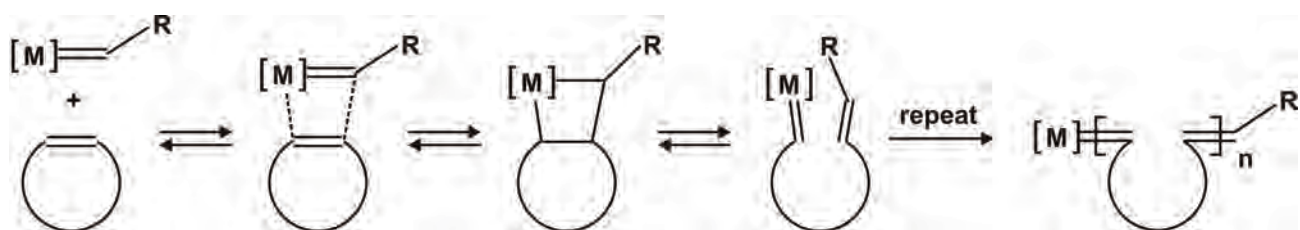


**Scheme 1.13:** Different ways to polymerise cycloalkenes.

The first example of ROMP dates back to 1955 when Anderson and Merckling patented a procedure to polymerise norbornene to a polymeric substance of unknown structure.<sup>73</sup> The catalyst for the ROMP reaction was formed *in situ* by mixing titanium(IV) chloride with reducing agents such as alkylated metals. The structure of this polymer remained unknown until 1960 when norbornene was polymerised with a combination of titanium(IV) chloride and lithium aluminium tetraheptyl.<sup>74</sup> The results of infrared spectroscopy and ozonolysis of the polynorbornene pointed to an unsaturated polymer that contained cyclopentane rings and led to the conclusion that polymerisation occurred through a type of ring-opening polymerisation.<sup>74</sup>

### 1.5.2. Mechanism of ROMP

ROMP of cycloalkenes is catalysed by transition metal alkylidenes. The general mechanism of the reaction is based on the original mechanism proposed for olefin metathesis (**Scheme 1.14**).<sup>75</sup> Initiation starts with the coordination of a cycloalkene to a metal alkylidene complex. A subsequent [2+2] cycloaddition reaction yields a four-membered metallacyclobutane intermediate. Cycloreversion of this strained intermediate affords a metal alkylidene of increased size due to the incorporation of the cycloalkene monomer. During propagation the above-mentioned steps are repeated to facilitate the growth of the polymer chain. Propagation continues until the monomer is depleted, equilibrium is reached or the reaction is terminated by the deliberate addition of a quenching agent. ROMP with ruthenium carbene catalysts is generally terminated with ethyl vinyl ether, which replaces the transition metal at the end of the polymer with a methylidene group.

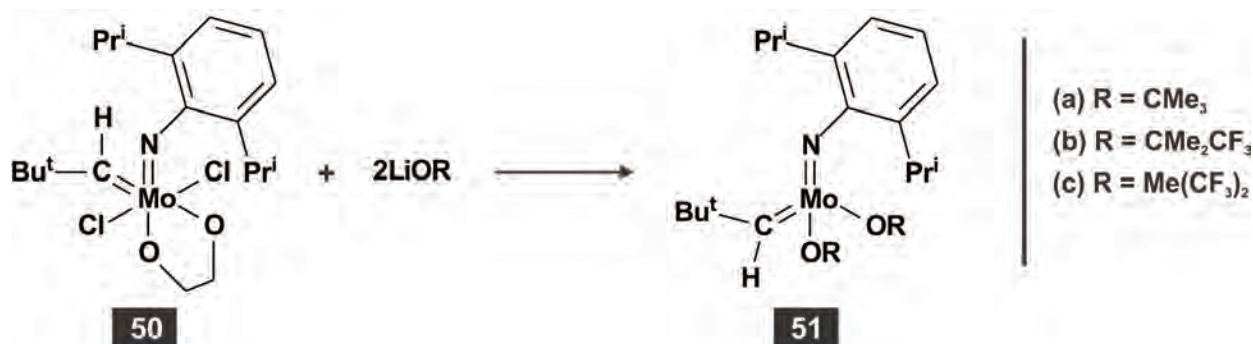


**Scheme 1.14:** General mechanism of ROMP of cycloalkenes.<sup>76</sup>

### 1.5.3. Development of well-defined ruthenium carbene ROMP catalysts

The original catalysts used for ROMP were generated *in situ* from a halide or oxide of an early transition metal such as W, Mo Rh or Ru and an alkylating agent (Lewis acid) such as  $R_4Sn$  or  $AlCl_3$ .<sup>77</sup> Examples of these classical catalysts include  $WCl_6/BuLi$ ,<sup>78</sup>  $MoCl_5/SnPh_4$ <sup>79</sup> and  $ReCl_5/Bu_4Sn$ .<sup>80</sup> Classical catalytic systems are widely used in the commercial application of ROMP due to their low cost and simplicity of preparation.<sup>77</sup> However, the harsh reaction conditions that are required often cause a lack of reaction control that consequently limits the utility of such catalysts.<sup>81</sup>

Improved understanding of the mechanistic aspects of metathesis and the successful synthesis of metal carbene complexes by Fischer<sup>82</sup> and Schrock<sup>83</sup> paved the way for the development of highly active single-component homogeneous catalysts. These catalysts are characterised by fast initiation, high catalytic activity and a high degree of reaction control that allows precise adjusting of molecular weight and polydispersity.<sup>3</sup> An early example of the application of a metal carbene in metathesis chemistry is  $(CO)_5W=CPh_2$  that was used in the ROMP of 1-methylcyclobutene.<sup>84</sup> An important advance was made when the research group of Schrock reported the synthesis of a series of molybdenum carbene complexes (**Scheme 1.15**).<sup>85</sup> The molybdenum carbene complex **51c** has been used to affect the living ROMP of functionalised norbornenes that do not contain active protons.<sup>86</sup> Although molybdenum carbene catalysts are highly active, they suffer from extreme air and moisture sensitivity and require special handling techniques.<sup>81</sup> The oxophilic nature of early transition metal catalysts limits their functional group tolerance and reduces the number of potential substrates.<sup>87</sup>



**Scheme 1.15**<sup>85</sup>: Well-characterised olefin metathesis catalysts that contain molybdenum.

The efficiency of metathesis catalysts can be described in terms of their selectivity, activity, and stability.<sup>88</sup> An analysis of the experimental work published in the field of metathesis chemistry suggested that catalysts based on late transition metals would be best suited for the metathesis of alkenes.<sup>89</sup> Metal complexes based on ruthenium showed superior functional group tolerance

combined with the highest selectivity for alkenes over other functionalities. Subsequently, the synthesis of the first well-defined ruthenium alkylidene complex **52** was reported.<sup>90</sup> This complex was an efficient catalyst for the ROMP of norbornene and other highly strained cycloalkenes but lacked activity towards low-strain monomers. In an attempt to broaden the activity of **52**, the ruthenium alkylidene complexes **53** and **54** were synthesised (Figure 1.1).<sup>91</sup> The catalytic activity of these complexes increases with the basicity of the phosphines ( $\text{PPh}_3 \ll \text{PPR}_3^i < \text{PCy}_3$ ).

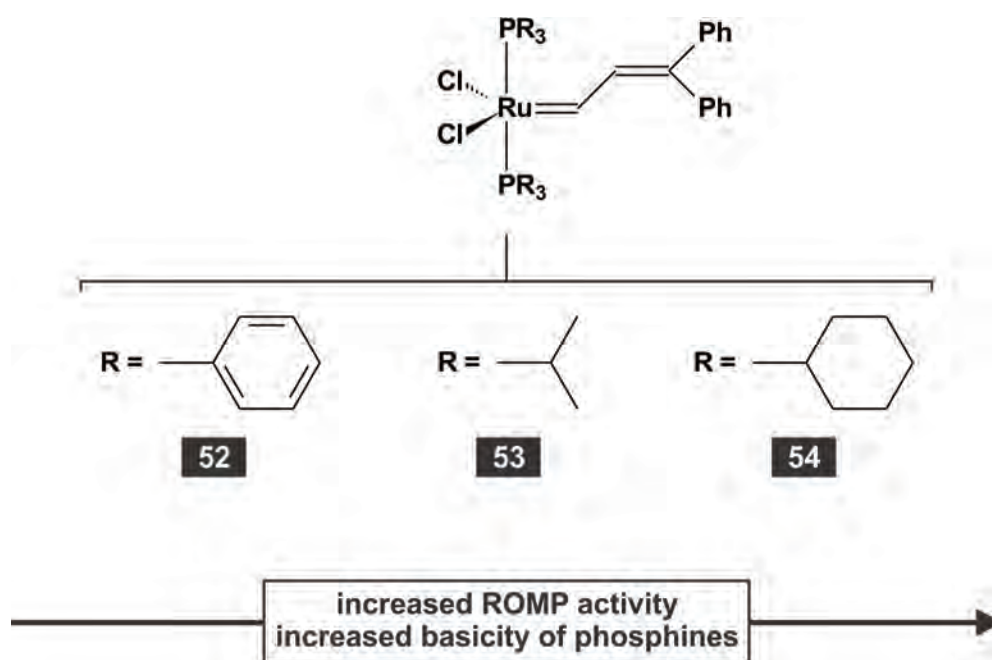


**Figure 1.1**<sup>91</sup>: Variations on the first well-defined ruthenium alkylidene complex.

Although **54** was able to catalyse the ROMP of lower strain monomers, such as cyclopentene, it was the synthesis of **55**<sup>92</sup> (Grubbs-I) that initiated the rapid expansion of the chemistry of well-defined ruthenium carbene catalysts.<sup>4,93</sup> Following the success of **55**, a second generation catalyst **56**<sup>94</sup> (Grubbs-II) was synthesised using **55** as starting material. This N-heterocyclic carbene complex combined activity superior to that of **54** and **55** with air, water and functional group tolerance.<sup>94</sup> Grubbs-II catalysed the ROMP of low-strain and sterically demanding monomers<sup>95</sup> as well as the ring-closing metathesis<sup>96</sup> (RCM) and cross metathesis<sup>97</sup> (CM) of sterically demanding substrates. This kind of reactivity was previously only possible with early transition-metal catalysts.



#### 1.5.4. Thermodynamics of ROMP

ROMP, like all other chemical reactions, occurs only if the Gibbs free energy change ( $\Delta G$ ) is negative under the prevailing reaction conditions. In general, the value of the entropy change ( $\Delta S$ ) is negative for ring-opening polymerisation due to the loss of translational entropy.<sup>98</sup> It can be concluded from the fundamental equation  $\Delta G = \Delta H - T\Delta S$  that the reaction will only be favourable when the positive entropy term ( $-T\Delta S$ ) is balanced by a sufficiently large and negative enthalpy change ( $\Delta H$ ).

Extensive thermodynamic studies have revealed a correlation between  $\Delta H$ , ring strain and the polymerisability of small-ring cycloalkenes.<sup>71</sup> Increased ring size is associated with a decrease in the values of  $\Delta H$  and ring strain approaching zero for large rings. Despite this situation, it is observed that ROMP of cycloalkenes with large rings may be favourable due to a positive entropy change. In general, ROMP is observed for cycloalkenes with three, four, eight or more carbon atoms in the ring. These monomers possess a considerable amount of strain ( $>5 \text{ kcal}\cdot\text{mol}^{-1}$ ) that results in high conversion to polymers. Examples of such monomers include cyclobutene, *cis*-cyclooctene, norbornene, and norbornene derivatives.<sup>99</sup> Due to the low ring strain of five-, six- and seven-membered cycloalkenes, ROMP of these compounds is crucially dependant on reaction temperature, concentration of the monomer, substituents at the ring and whether the alkene is part of a mono-, bi- or multicyclic ring system.<sup>98</sup> Bridged cycloalkenes, such as norbornene, exhibit increased ring strain that enable them to take part in ROMP. However, it can be anticipated that the polymerisability of polycyclic and cage alkenes will also depend on the steric bulk of the specific monomer and that this factor could exclude even sufficiently strained monomers from successful ROMP.

ROMP is typically a thermodynamically controlled process that leads to the establishment of equilibrium between monomeric and polymeric species. The equilibrium monomer concentration  $[M]_{\text{eq}}$  is related to the reaction temperature by **equation 1**.<sup>100</sup>

$$\ln[M]_{\text{eq}} = \frac{\Delta H_{\text{p}}^{\circ}}{RT} - \frac{\Delta S_{\text{p}}^{\circ}}{R} \quad \mathbf{1}$$

For a particular ROMP reaction at temperature **T** there is a minimum monomer concentration  $[M]_{\text{eq}}$  without which polymerisation will not be observed. Conversely, a given monomer concentration will be associated with a temperature above which polymerisation will not take place.<sup>100</sup> The equation shows that an increase in the enthalpy (ring strain) or the initial monomer concentration will increase the polymer yield. The conditions for successful addition polymerisation have been summarised by Ivan and is shown in **Table 1.1**.<sup>98</sup> It can be concluded from the above-mentioned discussion that polymer synthesis at low temperature and high monomer concentration can offset

an unfavourable entropy term and thus constitutes the best experimental strategy when attempting to synthesise polymers from unfamiliar monomers.

**Table 1.1: Thermodynamic parameters for ROMP as a function of monomer ring size<sup>x</sup>**

Ring size	$\Delta H$	$T\Delta S$	$\Delta G$	$[M]_{eq}$	Extent of polymerisation
3	Large negative	Small negative	Large negative	Very low	Essentially complete.
4					
5	Small or zero	Small negative	Small, negative or positive <sup>ii</sup>	0.01 – 5 mol-dm <sup>-3</sup>	Partial or no reaction
6					
7					
8	Similar to 3- and 4-membered rings.				
9					
10					
Very large	Zero	Positive	Negative	Low	High, Entropy driven.
<sup>x</sup> Under normal conditions of concentration, temperature and pressure.					
<sup>y</sup> Sign and magnitude very sensitive to the nature of the ring, to substituents, and to the reaction conditions.					

## 1.6. Cage polymers

### 1.6.1. Introduction

Polymers obtained from cage alkenes may be classified according to the position of the cage structure within the polymer (**Figure 1.2**). In the first type, the cage compound is a pendant group that does not form part of the backbone of the polymer. By contrast, backbone cage polymers contain cage structures as part of the main polymer framework.

### 1.6.2. Structure-property relations in polymers

The principles of polymer science may be found in standard textbooks on the topic.<sup>101-103</sup> It is clear from these texts that intricate links exist between the chemical compositions and physical properties of polymers. Polymer properties are related not only to the chemical nature of the polymer, but also to such factors as extent and distribution of crystallinity, distribution of polymer chain lengths, and nature and amount of additives.<sup>101</sup> These factors influence essentially all the polymeric properties to some extent including hardness, flammability, chemical stability, biological response, moisture retention, appearance, dyeability, softening point, and electrical properties.

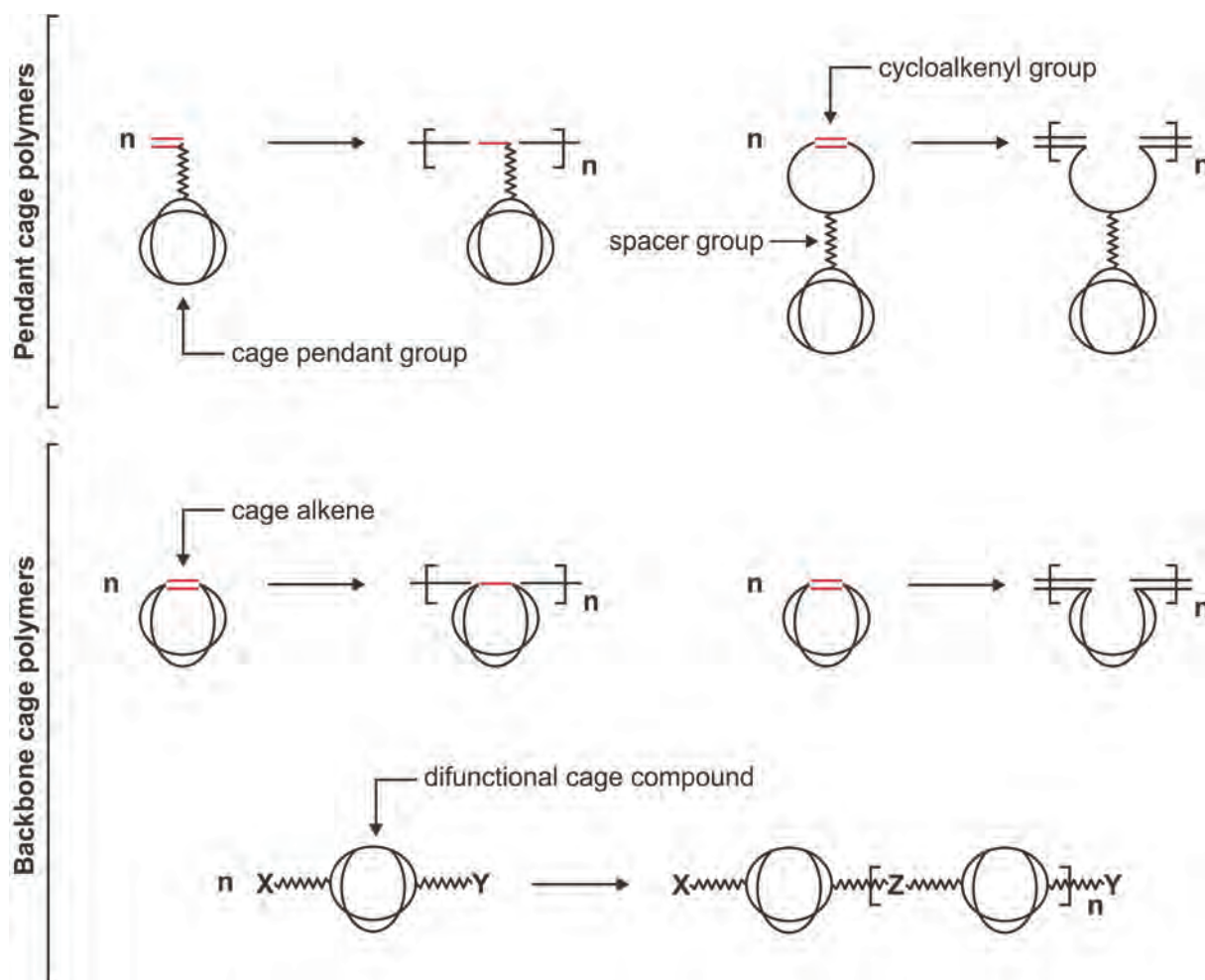


**Figure 1.2:** A classification of cage polymers.

Some of the properties most frequently reported for polymers are summarised in **Table 1.2**<sup>101-103</sup>. The effects of some structural features on the properties of polymers are summarised in **Table 1.3**.

**Table 1.2: Commonly reported properties of polymers**

Property	Significance
<b>Polydispersion index (PDI)</b>	The PDI expresses the degree of uniformity of the polymer chain lengths formed during the polymerisation process. A PDI is the ratio of the mass average molecular mass <sup>a</sup> ( $M_w$ ) and the number average molecular mass ( $M_n$ ). When a PDI value is unity, the polymer is monodisperse. In practice $1 \geq \text{PDI} \leq 2$ indicates a fairly uniform distribution of polymer chain sizes for synthetic polymers. Polymers with more uniform chain lengths are desirable since it leads to more uniform properties.

<sup>a</sup> This term is also known as the **weight average molecular weight**.

Table 1.2 - continued

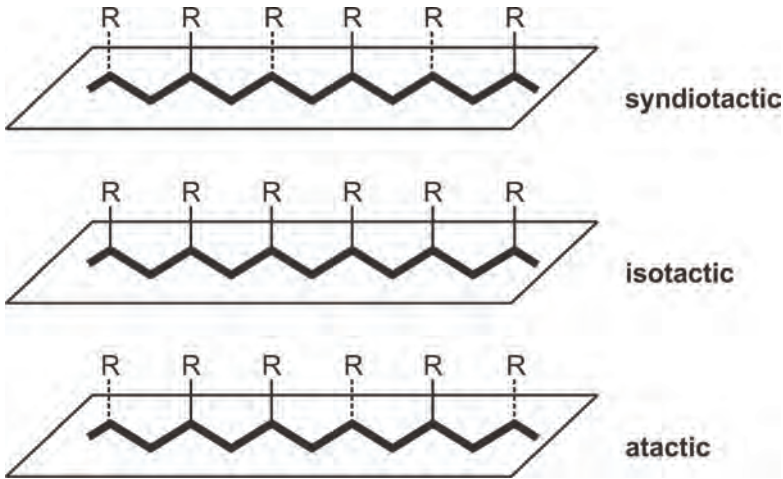
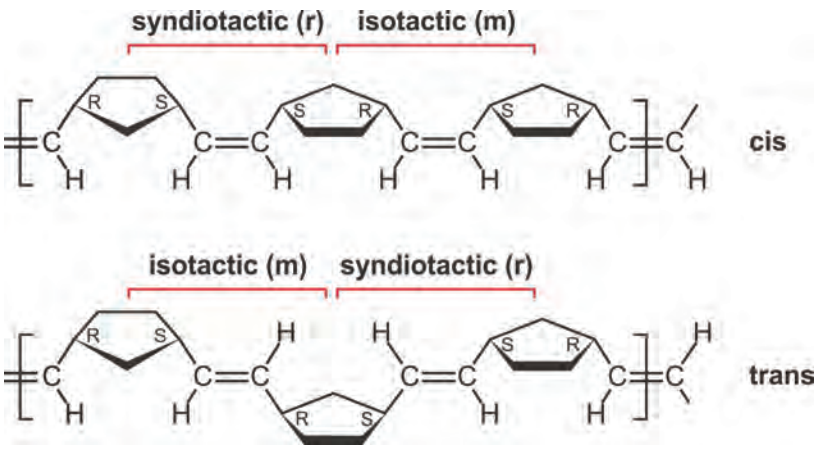
Property	Significance
<p><b>Stereoregularity</b></p>	<p>The regularity in the configurations of successive stereocentres determines the tacticity of the polymer chain. Three configurations are distinguished for polymers formed from monosubstituted alkenes:<sup>102</sup></p>  <p>The regularity or lack of regularity in polymers affects their properties by way of large differences in their abilities to crystallise. Atactic polymers are amorphous, soft materials with lower physical strength. By contrast, the corresponding isotactic and syndiotactic polymers are usually crystalline materials due to their more ordered internal structures.</p>
<p><b>Stereoregularity</b></p>	<p>ROMP yields polymers where the double bond is retained in the product and possible variations in double bond stereochemistry must be considered with tacticity in the structural analysis. For example, in the case of polynorbornene four combinations of dyad tacticity and double bond stereochemistry are distinguished<sup>104</sup>:</p>  <p>It is important to note that different catalytic systems may produce polymers with different tacticities from the same monomer.</p>



Table 1.2 – continued

Property	Significance
<b>Crystallinity and crystalline melting point (<math>T_m</math>)</b>	A crystalline polymer is a polymer with an ordered structure. Polymers contain varying degrees of crystalline and non-crystalline or amorphous regions. The crystalline melting point is the melting temperature of the crystalline regions within a polymer sample. $T_m$ is not as sharp as those observed for substances composed of simple molecules. Crystallinity is favoured by high interchain forces, regular structure, high symmetry, increased stress, and homogeneous chain lengths. Crystalline polymers generally have lower opacity than amorphous polymers.
<b>Glass transition temperature (<math>T_g</math>)</b>	The glass transition temperature is the temperature range where a polymer gains local or segmental mobility. The polymer changes from a brittle to a more flexible material. Many polymer properties change at $T_g$ , including stiffness, refractive index, dielectric properties, gas permeability, x-ray adsorption, and heat capacity. $T_g$ increases with the presence of bulky pendant groups and stiffening groups, chain symmetry, polar groups, and cross-linking. $T_g$ decreases with the presence of additives, flexible main chain groups, non-polar groups, and dissymmetry.

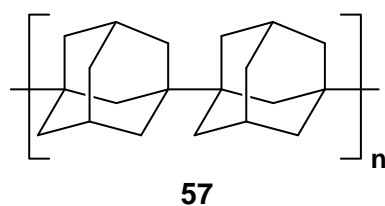
Table 1.3<sup>101</sup>: Some structure-property relations in polymers<sup>x</sup>

Property	Increased crystallinity	Increased molecular mass	Increased PDI	Addition of backbone stiffening groups
$T_g$	+	+	-	+
Softening point	+	+	-	+
Chemical resistance	+	+	-	+
Brittleness	-	+	+	+
Tensile strength	+	+	-	+
Toughness	+	+	+	+

<sup>x</sup> Key: + = increase; 0 = little or no effect; -- = decrease in property.

### 1.6.3. Survey of cage polymers

Polyadamantane (**57**) was the first polymer that included a cage compound as part of the polymer backbone.<sup>105</sup> The polymer is a white powder with a melting point of more than 420°C. It was concluded from x-ray diffraction data that the polymer had a degree of crystallinity in excess of 80%. Since this time adamantane has been used as a pendant group and included into the backbone of a wide variety of polymers.<sup>106</sup>



### 1.6.3.1. Cage pendant polymers from vinyl polymerisation

Adamantane has been used as a pendant group in a number of methacrylates. Matsumoto *et al.*<sup>107</sup> investigated the kinetics of the free radical polymerisation of **58a** – **58e** with various free radical initiators at 60°C in benzene (**Figure 1.3**). Polymerisation of the bulky monomers **58d** and **58e** increased the polymerisation rate and the average molecular mass of the polymer when compared to the methacrylates obtained from **58a** – **58c**. The result has been ascribed to a decrease in the termination rate, resulting from an increase in the concentration of the propagating polymer radical in the steady state.<sup>107</sup> Free radical polymerisation of **58d** yielded a predominantly syndiotactic polymer that did not show a  $T_g$  below the decomposition temperature (254 – 304°C). Identical polymerisation of **58e** gave a polymer of similar tacticity with a  $T_g$  of 194°C. A predominantly isotactic polymer prepared from **58d** by anionic polymerisation showed a  $T_g$  of 183°C.<sup>108</sup> The observed  $T_g$  values of these polymers were higher than for any methacrylate reported up to that point. Compare, for example the  $T_g$  range of 56 – 78°C reported for polycycloalkylmethacrylates.<sup>109</sup>

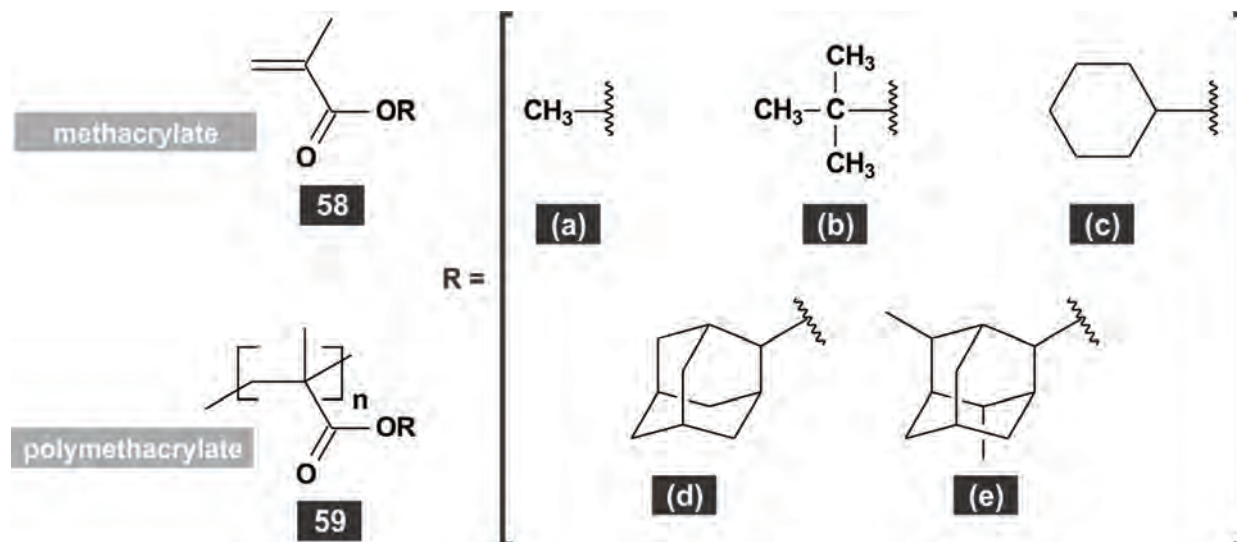
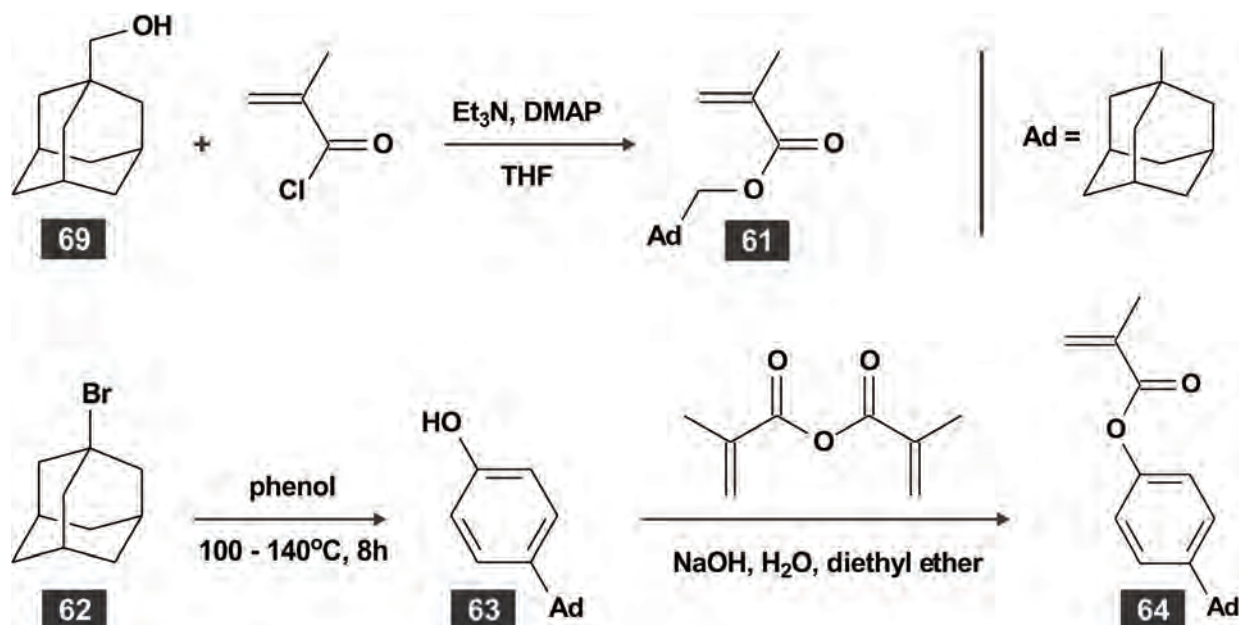


**Figure 1.3:** Adamantane-containing methacrylate monomers.

Mathias *et al.*<sup>7</sup> investigated the influence of a spacer group between the main polymer chain and the adamantyl groups. The monomers **61** and **64** were synthesised (**Scheme 1.16**) and then polymerised under free radical conditions. It was found that the homopolymers of **61** and **64**

showed approximately the same tacticity as polymethylmethacrylate so that the enhancement of  $T_g$  could be ascribed to the nature of the spacer group. The polymers derived from **61** and **64** had  $T_g$  values of 201°C and 253°C, respectively.

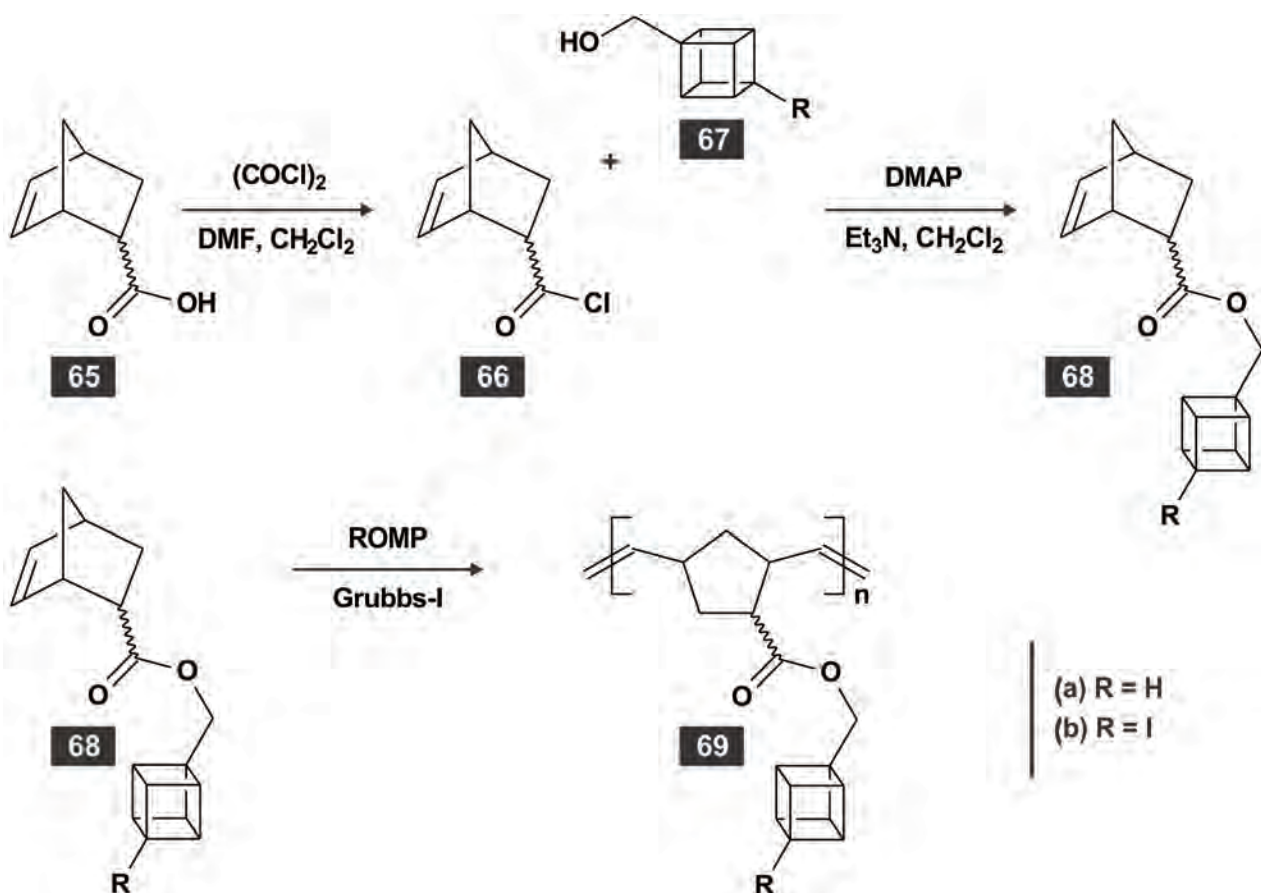


**Scheme 1.16**<sup>7,110</sup>: Adamantane-containing methacrylate monomers with spacer groups.

### 1.6.3.2. Cage pendant polymers from ROMP

Priever *et al.*<sup>6</sup> prepared and polymerised the norbornene derivative **68** (**Scheme 1.17**). The commercially-available *endo-exo* mixture of 5-norbornene-2-carboxylic acid (**65**) was converted<sup>111</sup> to the corresponding acid chloride **66** by treatment with oxalyl chloride. The reaction between **66** and cubylcarbinol (**67a**) or 1-iodo-4-(hydroxymethyl)cubane (**67b**) produced the norbornene esters **68a** and **68b**.

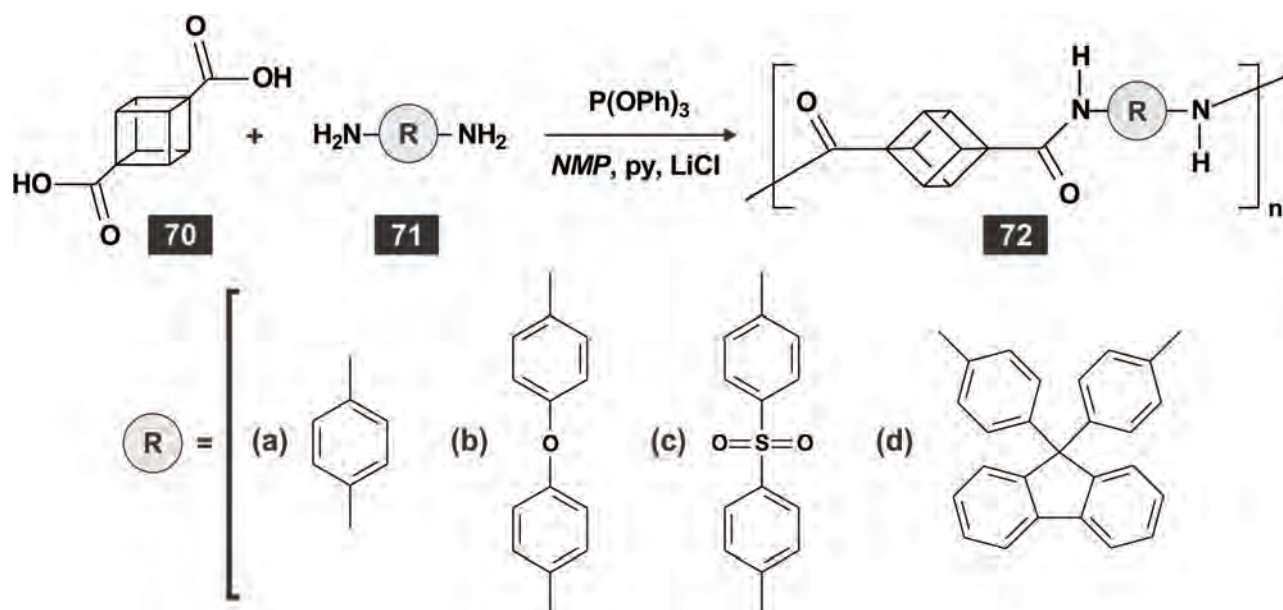
Subsequent polymerisation of **68** with Grubbs-1 (**55**) in THF under nitrogen for 24 hours at room temperature yielded polymers **69a** and **69b** upon precipitation with pentane.<sup>6</sup> A low monomer-to-catalyst ratio yielded polymers of relatively low molar masses ( $M_n \sim 3 \times 10^4$ ). The PDI values for **69a** and **69b** were 1.11 and 1.26, respectively. Neither polymer exhibited a glass transition or melting temperature. TGA revealed that **70a** decomposed when heated above 383°C. The loss of mass corresponded to the loss of the carboxyl and cubane groups. Polymer **69b** behaved similarly at 250°C. Both polymers exhibit significant solvent solubility and behaved thermally like simple cubane derivatives.



**Scheme 1.17**<sup>6</sup>: Synthesis and polymerisation of cubane-containing ROMP monomers.

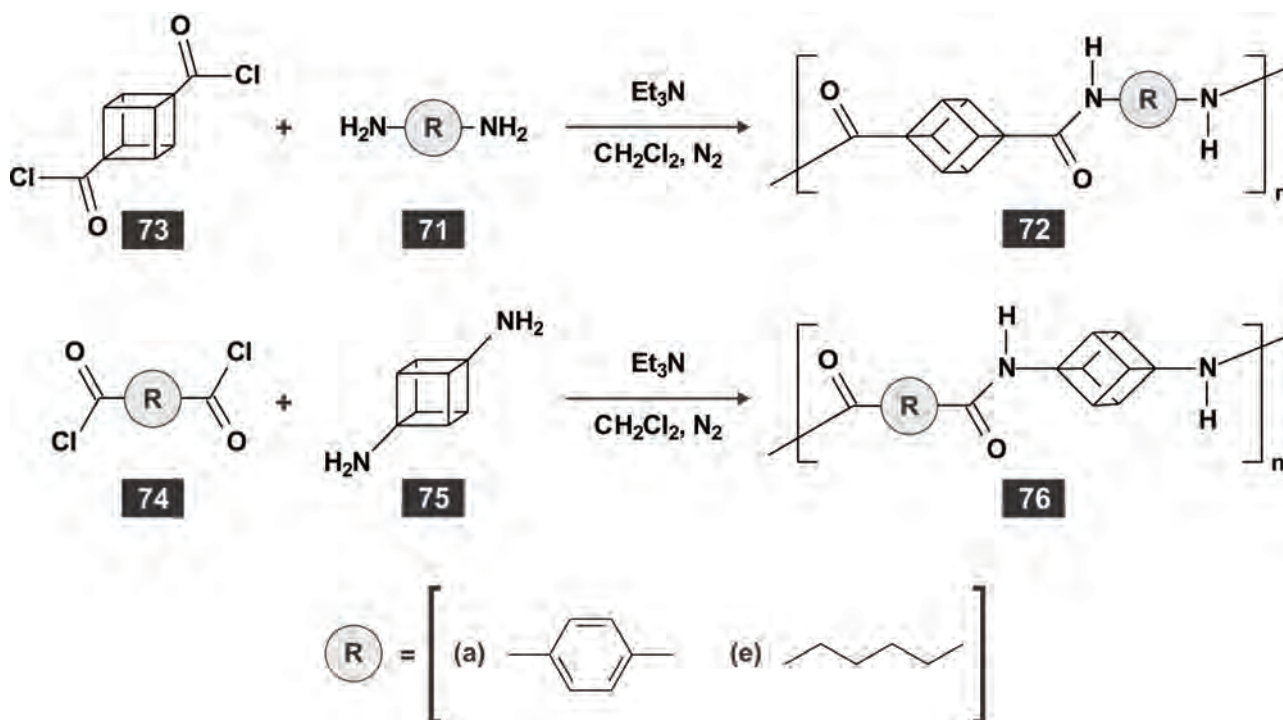
### 1.6.3.3. Backbone cage condensation polymers

Kakuchi *et al.*<sup>112</sup> reported the first examples of condensation polymers containing cubane units in the backbone. A method previously described to polymerise aromatic diacids and diamines was applied to cubane-1,4-dicarboxylic acid (**70**) and various aromatic diamines (**Scheme 1.18**). The reaction was conducted in the presence of an aryl phosphite, an organic base, and an inorganic salt.<sup>113</sup> The latter was added to improve the solubility of the polymer and maximise the molecular mass. The yield of polyamide was almost quantitative in each case. This method of polymerisation yielded polymers with relatively low molar masses ( $\sim 3 \times 10^4$ ) and high PDI-values ( $> 2.4$ ).<sup>113</sup> The polycondensation system for 1,4-phenylenediamine (**71a**) rapidly turned heterogeneous and the polyamide **72a** precipitated from the reaction mixture.<sup>112</sup> The other systems remained homogeneous. Polyamide **72a** showed extremely low solubility in organic solvents. Analysis of this polymer with x-ray diffraction indicated a high degree of crystallinity. The high degree of crystallinity and poor solubility of **72a** was ascribed to a rigid and rod-like backbone structure.<sup>112</sup> In contrast, polymer **72d** exhibited good solubility in a variety of organic solvents due to a bulky structure that prevents significant intermolecular hydrogen bonding.



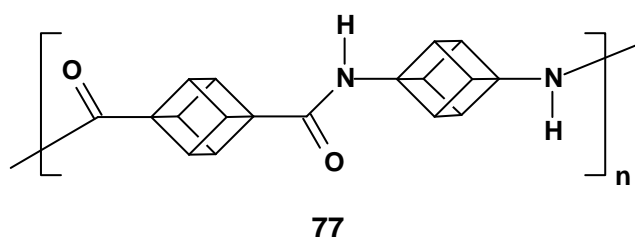
**Scheme 1.18**<sup>112</sup>: Synthesis of cubane-containing condensation polymers.

Mahkam and Sanjani<sup>114</sup> synthesised a number of cubane-containing polyamides (**Scheme 1.19**). This synthesis procedure is similar to the well-known nylon rope trick used in chemical demonstrations. Polymers with relatively low molar masses ( $\sim 1.5 \times 10^4$ ) were obtained. No glass transition temperatures or melting points were observed, but the onset of decomposition was noted in the temperature range  $175^\circ\text{C} - 280^\circ\text{C}$ .<sup>114</sup>



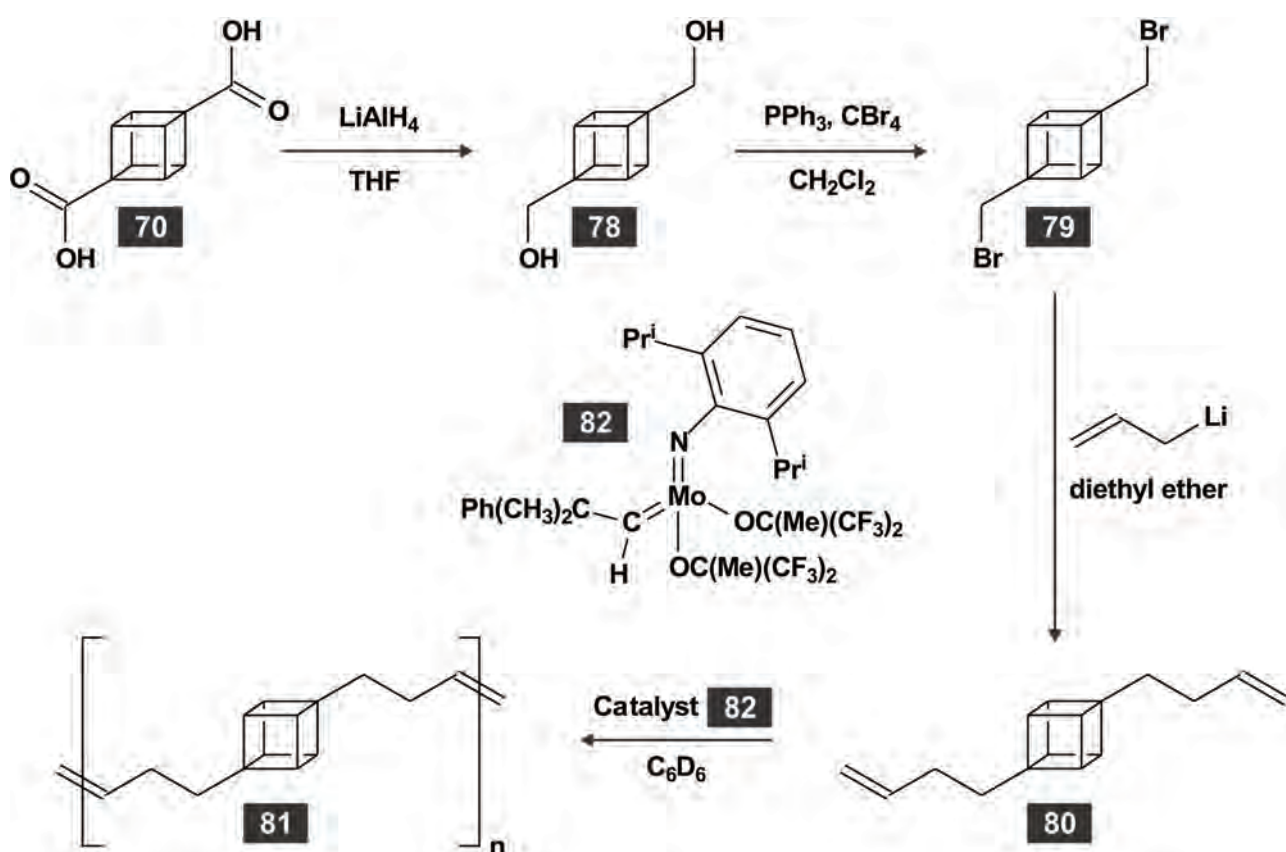
**Scheme 1.19**<sup>114</sup>: Synthesis of polyamides.

The reaction of cubane-1,4-dicarbonyl chloride (**73**) with 1,4-diaminocubane (**75**) is of particular interest due to the high content of cubane units in polycubylcubanamide (**77**). The resulting polymer was obtained in 94% yield and contained an average of 43 repeating units.<sup>114</sup>



#### 1.6.3.4. Backbone cage polymers from metathesis reactions

Chauvin and Saussine<sup>5</sup> reported a cubane-containing polymer prepared by acyclic diene metathesis (ADMET<sup>115</sup>) polymerisation (**Scheme 1.20**).

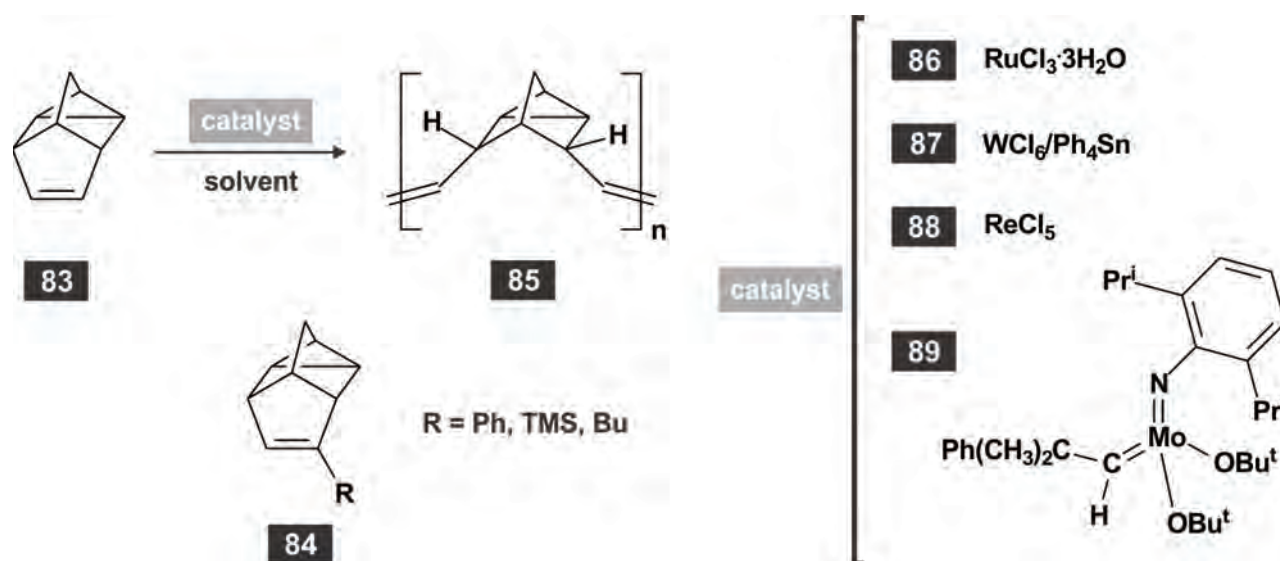


**Scheme 1.20**<sup>5,116</sup>: Preparation of backbone cage polymers by ADMET polymerisation.

1,4-Bis(bromomethyl)cubane (**79**) was prepared from cubane-1,4-dicarboxylic acid (**70**) according to a method reported by Eaton and Yip.<sup>116</sup> Treatment of **79** with allyllithium<sup>117</sup> yielded the monomer 1,4-bis(homoallyl)cubane (**80**), which was subsequently polymerised in the presence of the

Schrock molybdenum alkylidene catalyst **82**. This technique afforded the oligomer **81** with 6 – 7 repeat units. The authors attributed the lack of chain growth to lack of solubility.<sup>5</sup> Analysis of the oligomer with DSC did not reveal a  $T_g$  or any other transition, but an exothermic peak in the region 180 – 260°C indicated the decomposition of the material. An attempt was made to improve the solubility of the polymer by co-polymerisation of **80** and 1,4-butadiene.<sup>5</sup> The resulting material was soluble in a variety of organic solvents including benzene, THF and chloroform. Analysis of the crude co-polymer with GPC showed a broad molar mass distribution in the 250 – 2200 range. The presence of several peaks in the GPC-trace was ascribed to the presence of a mixture of homopolymers and co-polymers.<sup>5</sup> Purification of the mixture yielded a co-polymer with a PDI of 1.8 and an average of 14 repeat units.

Lautens *et al.*<sup>11,118-119</sup> investigated the ROMP of deltacyclene (**83**) and substituted deltacyclenes (**84**) with different catalysts (**Scheme 1.21**). Deltacyclenes are highly strained cage alkenes prepared by the catalytic reaction of norbornadiene and acetylenes.<sup>120</sup> Polymerisation reactions focused on **83**, since the substituted deltacyclenes failed to undergo ROMP to any appreciable extent.



**Scheme 1.21:** Preparation of backbone cage polymers by ROMP.

ROMP of deltacyclene (**83**) were carried out with 1 mol %  $\text{RuCl}_3 \cdot 3\text{H}_2\text{O}$  in anhydrous ethanol at 60°C.<sup>11</sup> The reaction yielded a polydeltacyclene (**85**) of low molecular mass that precipitated from solution. The molecular mass was increased significantly by the addition of water to the reaction mixture as well as by an increase in the monomer-to-catalyst ratio (**Table 1.4**). It was noted that the PDI of **85** increased with increasing water content, i.e. PDI = 2.04 (ethanol) and 3.46 (water). The polymers were soluble in a number of organic solvents, including halogenated solvents, THF, cyclohexane, benzene, and xylenes.

**Table 1.4<sup>11</sup>: Effect of water and monomer-to-catalyst ratio on polymerisation**

Entry	Ratio (mol)		Molecular mass	Yield (%)	Ratio
	Monomer: Catalyst	EtOH: H <sub>2</sub> O			<i>cis</i> : <i>trans</i>
1	100: 1	1: 0	2 000	31	1: 1.3
2	100: 1	1: 1	103 000	72	1: 1
3	100: 1	1: 100	206 000	90	1: 1.5
4	100: 1	0: 1	207 000	85	1: 1.5
5	200: 1	1: 1	447 000	78	1: 1
6	600: 1	1: 1	856 000	85	1: 1

The *cis-trans* ratios of the polymers were determined from NMR data.<sup>11</sup> Signals corresponding to the olefinic protons in the *cis*- and *trans*-isomers were identified on the <sup>1</sup>H NMR spectrum. Integration of these signals provided the ratios reported in **Table 1.4**. Similarly, signals that correspond to the *cis*- and *trans*-isomers were identified in the <sup>13</sup>C NMR spectrum. Integration of these signals gave results in agreement with those from the proton spectra. The low stereoselectivity observed in polymerisations catalysed by **86** is in contrast to the reported *trans*-preference of ruthenium catalysts.<sup>121</sup> The authors made several attempts to improve the stereoselectivity of the ROMP reaction, but these did not change the results.

Lautens *et al.*<sup>118</sup> reported the influence of employing different catalysts on the stereoregularity of **85** (**Scheme 1.21**). Changing the catalyst to WCl<sub>6</sub>/Ph<sub>4</sub>Sn (**87**) affected the smooth transformation of the monomer to a polymer of approximately 70% *cis*-geometry. The polymer was of intermediate molecular mass ( $M_w = 20\ 000$ ) and was obtained in 73% yield. It was found that the catalyst ReCl<sub>5</sub> (**88**) was significantly more *cis*-stereoselective than **86** and **87**.<sup>118</sup> Polymerisation with **88** was carried out without solvent and afforded 48% of a polymer with >95% *cis*-geometry. GPC of the product indicated a polymer of high molecular mass ( $M_w = 986\ 000$ ). It was concluded from <sup>13</sup>C NMR data that a highly stereoregular polymer was obtained. Polymerisation of deltacyclene (**83**) with the Schrock molybdenum alkylidene catalyst **89** produced a white fibrous polymer in 90% yield.<sup>119</sup> NMR data showed that this polymer had predominantly *trans*-geometry that varied between 65 and 73%. The PDI values of high molecular mass polydeltacyclene (**85**) prepared with catalyst **89** had PDI values of 1.58 (no solvent,  $M_w = 466\ 000$ ) and 1.27 (toluene,  $M_w = 74\ 100$ ). The PDI value was improved to 1.09 by decreasing the molecular mass (toluene,  $M_w = 16\ 200$ ).

#### 1.6.3.5. Conclusions about the properties of cage polymers

Bulky monomers usually form rigid amorphous polymers. These polymers show high resistance to deformation and undergo very small elongations before rupturing.<sup>77</sup> Both the amorphous nature



and the high rigidity are due to the bulky side groups on the polymer chains resulting in high glass transition temperatures. The value of  $T_g$  is the most important single descriptor of amorphous polymers since the value of this parameter determines the type of use.<sup>122</sup> Values of  $T_g$  well above room temperature indicate rigid structural materials and those well below room temperature define the domain of elastomers.

Most of the available literature indicates that cage monomers have been incorporated into polymers as a means to modify the value of  $T_g$ . The value of  $T_g$  is known to increase with substituent size for rigid substituents.<sup>103</sup> It has also been shown that positioning the centre of mass of the substituent closer to the backbone and increasing the bulkiness of the substituent are important to increase the value of  $T_g$ .<sup>109</sup> Understanding the competing effects of rigidity, flexibility and the three-dimensional size of the cage monomer are important considerations when developing new cage monomers. **Table 1.5** lists some properties of cage polymers that may be derived from the examples in the previous section.

**Table 1.5: Properties of cage polymers**

General
<ul style="list-style-type: none"> <li>• Cage polymers are usually amorphous.</li> <li>• Cage polymers have high decomposition temperatures.</li> <li>• The inclusion of cage structures into polymers increases polymer rigidity.</li> </ul>
Pendant cage polymers
<ul style="list-style-type: none"> <li>• The inclusion of cage pendant groups into polymers increases <math>T_g</math> values.</li> </ul>
Backbone cage polymers
<ul style="list-style-type: none"> <li>• Backbone cage polymers frequently exhibit no thermal transitions values before polymer decomposition takes place.</li> <li>• Backbone cage polymers may exhibit varying degrees of crystallinity.</li> <li>• Backbone cage polymers prepared by condensation reactions are usually short-chained (small molar masses) with high PDI-values.</li> <li>• Backbone cage polymers prepared by condensation reactions tend to exhibit low solubility in non-polar solvents.</li> </ul>

## 1.7. Some applications of molecular modelling in organic chemistry

In recent years molecular modelling (computational chemistry) has developed into a useful tool to aid in predicting and explaining the outcomes of experimental results. The historical development and mathematical foundations of this field are available in a number of excellent publications.<sup>123-125</sup> Density functional theory<sup>126</sup> (DFT) was employed in this study. This section explains how the properties calculated with this computational technique were translated into useful explanations for chemical phenomena.

### 1.7.1. Potential energy surfaces, reaction pathways and geometric optimisations

The pathways available to a given set of reagents may be described by a potential energy surface (PES). As a consequence systematic evaluation of the surface yields information about the plausible reaction pathways that are available in the chemical system and the mechanisms of such reactions.<sup>127</sup> The PES provides a mathematical relation between the energy of a molecular system and small variations in its structure. A PES is usually multidimensional with the number of dimensions equal to the degrees of freedom within the molecule. The relation between energy ( $E$ ) and the geometric parameters ( $q_1, q_2, q_3 \dots$ ) is then given by  $E = f(q_1, q_2, q_3 \dots)$ . It is not possible to visualise a multidimensional surface in three-dimensional space. Therefore, a slice or slices are made through the multidimensional PES and the result represented in two or three dimensions. **Figure 1.4** shows a PES simplified to three dimensions.

Minima, maxima, and transition states are located at stationary points on the PES. At all these points  $\partial E / \partial q = 0$  for all geometric coordinates  $q$  along all directions. At the transition state  $\partial^2 E / \partial q^2 < 0$  in the direction of the reaction coordinate and  $\partial^2 E / \partial q^2 > 0$  along all other directions. At a minimum  $\partial^2 E / \partial q^2 > 0$  along all directions. A maximum can be recognised as a point where  $\partial^2 E / \partial q^2 < 0$  for all values of  $q$ . Chemical reactions should proceed from an energy minimum of the reactants to an energy minimum of the products along the path of lowest energy.<sup>128</sup> More than one reaction path may be available to the reagents and different energy minima on the surface correspond to different products to which the reagents may be transformed.

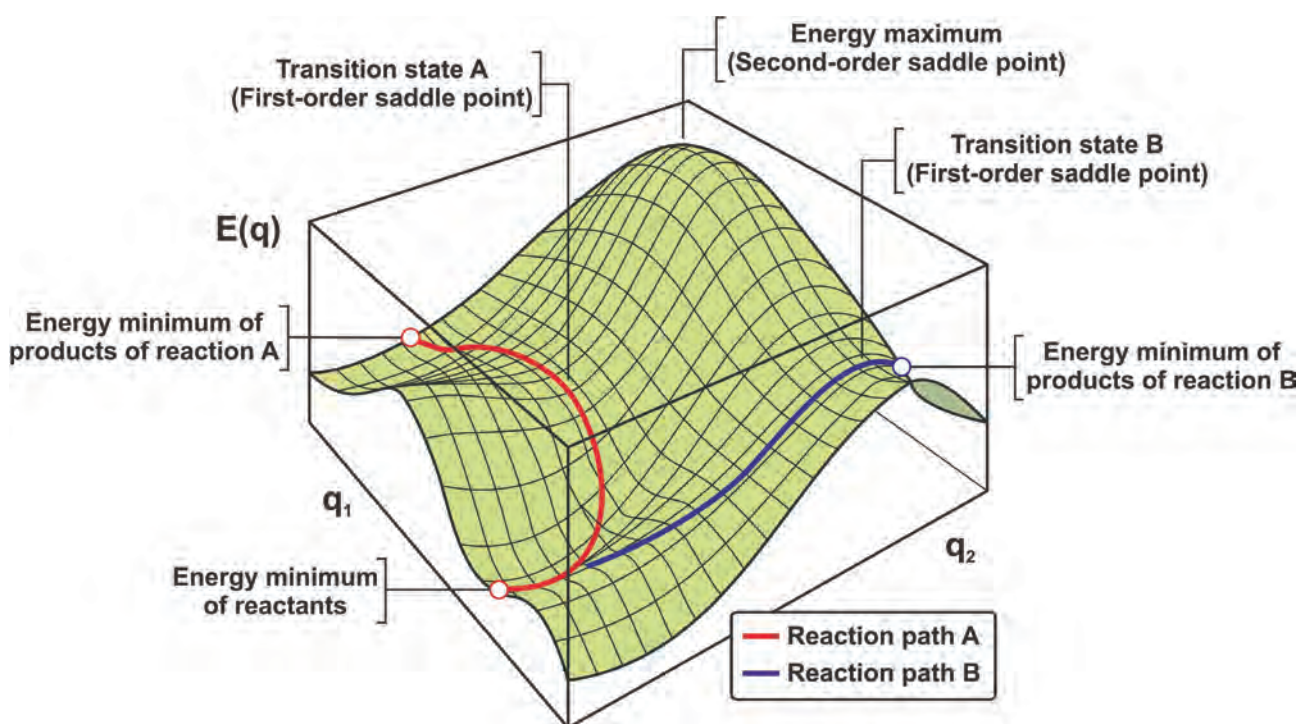


**Figure 1.4:** Recognising minima, maxima, and transition states on a PES.<sup>129</sup>

A PES can also be constructed for all possible conformations of a single molecule. The most stable conformation of a molecule is the one with lowest energy that is located at the global minimum of the PES. Although geometric optimisation algorithms attempt to find the global minimum, the minimum closest to the initial structure will be reported. Consequently, the initial structure should be a good guess. A conformational search can be used to verify that the energy of the structure obtained from a geometric optimisation is located at the global minimum.

Relatively little is known about the geometries of transition states and finding these are therefore generally more difficult than finding minima or maxima. The data for the transition states presented in this study were found from "chemical intuition" – a sensible initial structure was constructed followed by preliminary testing with a low cost semi-empirical calculation. Mathematically, transition states are first order saddle points on the PES (**Figure 1.4**). The structure associated with the first-order saddle point will exhibit one imaginary frequency and the normal mode of vibration associated with this frequency should emulate the motion of the atoms along the reaction coordinate. It is crucial to calculate the IR-spectrum of a suspected transition state to confirm that it has only one imaginary frequency and that the motions of the atoms agree with the mechanistic expectation of the modeller. This is done by animating the vibration at the imaginary frequency.

The simplest representation of a PES is obtained when only one slice is made through a multidimensional PES. The result is the commonly encountered two-dimensional energy diagram encountered in introductory chemistry textbooks. Frequently, only some important points on the multidimensional PES, such as the transition states and intermediates, are investigated and represented as a simplified energy diagram (**Figure 1.5**). Despite the simplification, such a diagram still provides valuable information regarding the chemical behaviour of a system.

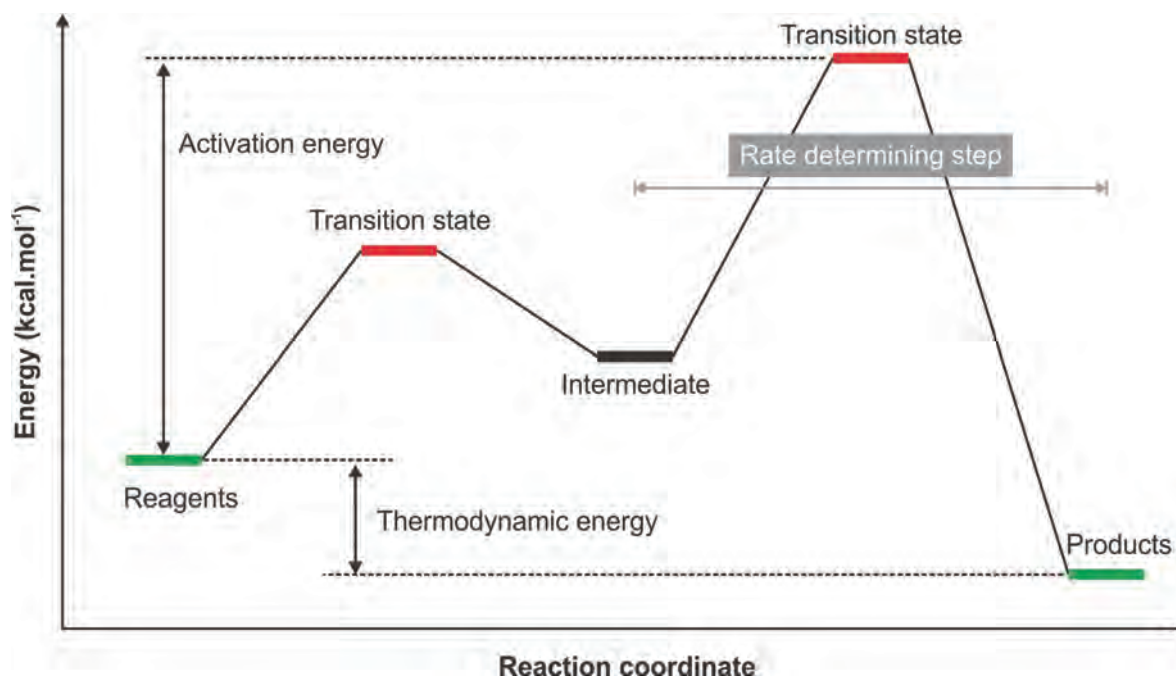


**Figure 1.5**<sup>129</sup>: A simplified two-dimensional PES.

## 1.7.2. Reactivity

A description of reactivities in terms of the molecular orbital theory requires information about the electronic structures of molecules. A convenient approach is to calculate the electronic properties of molecules with DFT and to interpret these data in terms of the frontier molecular orbital (FMO) theory. The FMO theory<sup>130-131</sup> is an approximation that holds that the most significant energy-lowering effect during a chemical reaction is from the combination of frontier molecular orbitals, i.e. the highest occupied orbital (HOMO) of one reagent and the lowest unoccupied orbital (LUMO) of the other reagent. Consequently only the HOMO-LUMO interactions need to be considered in the case of reacting neutral molecules. In the case of an ionic reaction the most important interaction is between the HOMO of the nucleophile and the LUMO of the electrophile (Figure 1.6).

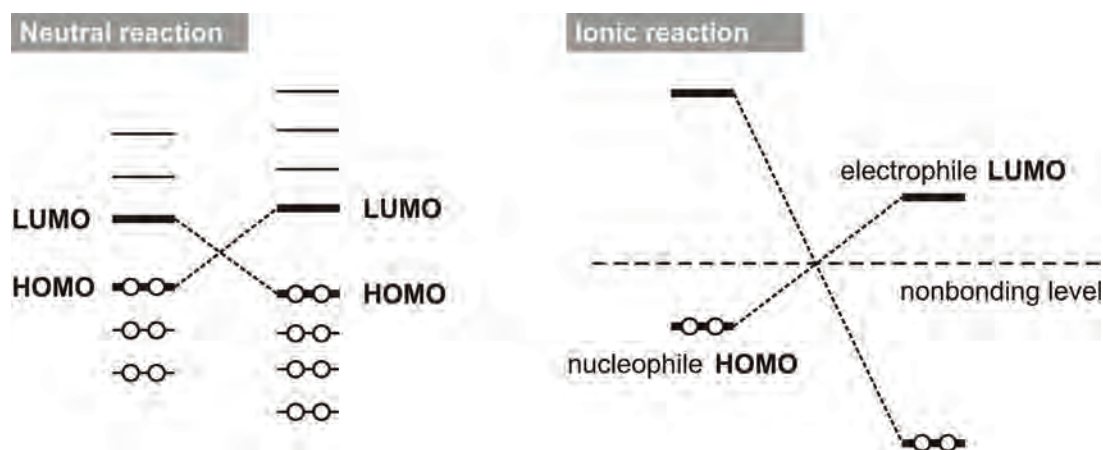


**Figure 1.6:** Generalised energy diagram for frontier orbital interactions.<sup>132</sup>

The FMO theory is an approximation and it is therefore important to consider the assumptions on which it is based. The FMO theory ignores interactions between filled orbitals and only interactions between frontier orbitals are considered. Also, the FMO theory strictly applies to the frontier orbitals in the transition state although the frontier orbitals of the reagents are frequently substituted. The assumptions indicated above cause some limitations when the FMO theory is used to interpret chemical reactivity. Firstly, molecular orbitals other than the frontier orbitals may influence the outcome of a chemical reaction when these have energies comparable to that of the frontier orbitals or if they are nonbonding. (Examples of such subjacent orbitals are the NHOMO and SLUMO, which refers to the next-to-highest occupied molecular orbital and the second lowest unoccupied molecular orbital, respectively.<sup>133</sup>) Also, electrostatic interactions may become dominant over HOMO-LUMO interactions when ions are involved or when the HOMO-LUMO energy gap is large. The factors considered when using the FMO theory as an interpretative tool in this work can be summarised as follows:<sup>134</sup>

1. The strength of the interaction between orbitals depends on the relative energy of the orbitals. A greater degree of interaction is observed when orbital energies are closely spaced. Thus, comparisons of the relative orbital energies should be of some use in predicting the relative importance of different possible interactions.
2. The strength of the interaction between orbitals depends on the achievable amount of overlap between them. The degree of overlap is influenced by how closely the orbitals can approach one another and by the shape, orientation, and size of the orbitals. The  $S_N2$  reaction between bromomethane and the hydroxide ion may serve as an example (**Figure 1.7**).

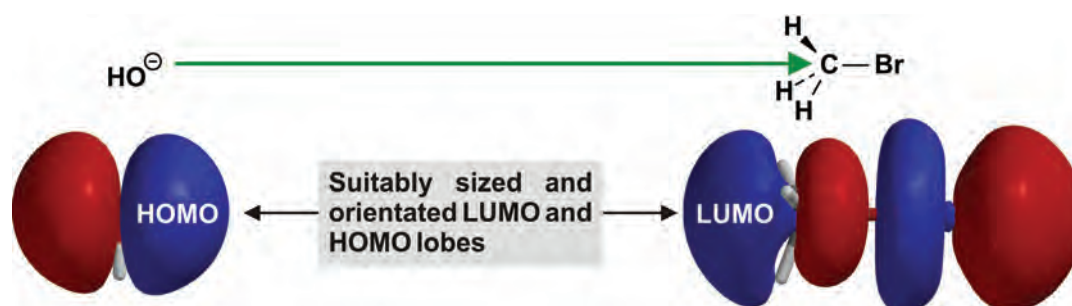


**Figure 1.7:** Reagents with favourably orientated HOMO and LUMO lobes.

Simultaneous representation of the total electron density and the LUMO of an electrophile may provide insight into the reactivity observed towards nucleophiles. A reaction is more probable when a suitably sized and orientated part of the LUMO protrudes from the surface of the total electron density. Different orbital pictures of propanol are presented in **Figure 1.8** to illustrate these ideas.

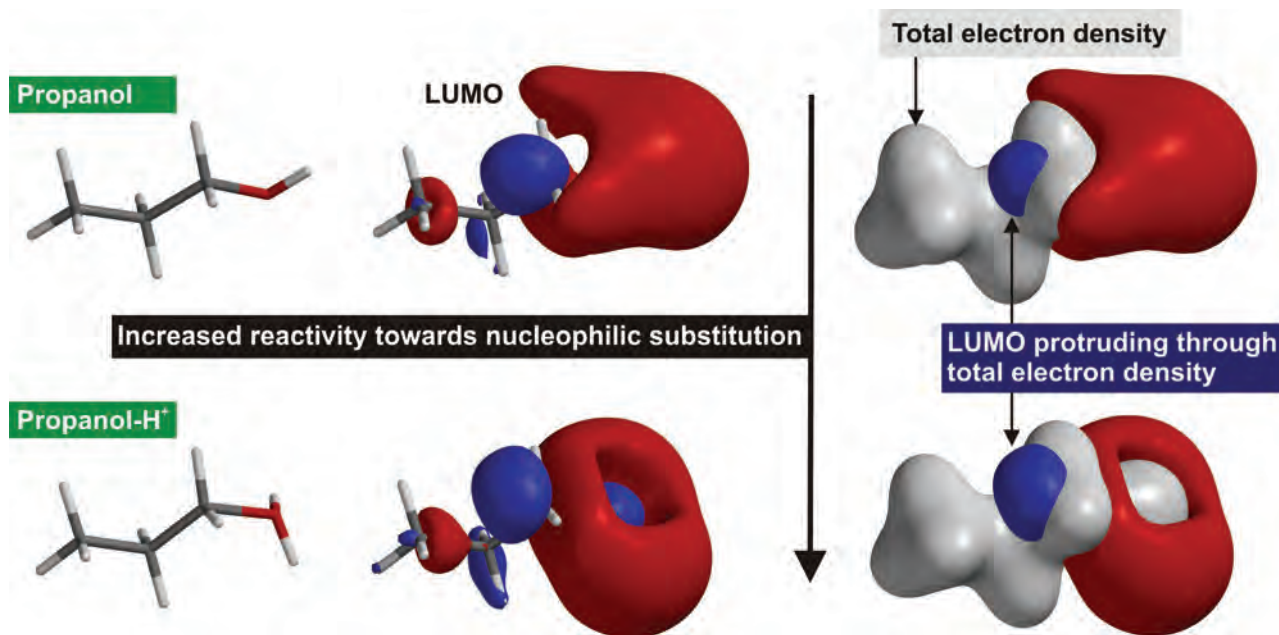


**Figure 1.8:** LUMO lobes protruding from the total electron density.

Since the hydroxyl group is not a good leaving group, acid catalysis is required in the nucleophilic substitution reactions of alcohols.<sup>135</sup> The increased reactivity of protonated propanol manifests as an increase in the size of the LUMO protruding through the total electron density at the  $\alpha$ -carbon atom (**Figure 1.8**). Small or absent protrusions may indicate that reactions with nucleophiles are unlikely at that particular point in a molecule.